GIUH model approach for the ungauged Achumani catchment using GIS techniques. A case study in La Paz, Bolivia

Espejo Rospigliossi Airthon Angel
February, 2009

GIUH model approach for the ungauged Achumani catchment using GIS techniques. A case study in La Paz, Bolivia

by

Airthon Espejo R.

Thesis submitted to the International Institute for Geo-information Science and Earth Observation in partial fulfilment of the requirements for the degree of Master of Science in Geo-information Science and Earth Observation, Specialisation: Water Resources and Environmental Management

Thesis Assessment Board

Dr. Ir. C.M.M. Mannaerts	(Chairman)	University of Twente
Dr. Ir. M.J. Booij	(External examiner)	University of Twente
Msc. Ir. Gabriel Parodi	(1st supervisor)	ITC, Enschede
Dr. Dinand Alkema	(2nd supervisor)	ITC, Enschede

INTERNATIONAL INSTITUTE FOR GEO-INFORMATION SCIENCE AND EARTH OBSERVATION
ENSCHEDE, THE NETHERLANDS

Disclaimer

This document describes work undertaken as part of a programme of study at the International Institute for Geo-information Science and Earth Observation. All views and opinions expressed therein remain the sole responsibility of the author, and do not necessarily represent those of the institute.

To my parents…

…my only and ever source of inspiration…

Abstract

The main objective of this thesis is to develop the GIUH to assess its performance for the Achumani catchment (La Paz, Bolivia). Three major stages were defined in order to develop the input data for the GIUH modelling process. The first stage consists in the data collection during the field work period. All the basic and only information for the Achumani catchment was collected (pluviographic, pluviometric and discharge data). Additionally, field survey was made for GCP collection for the drainage definition and topographic survey for calibration purposes. The second stage includes the hydrology analysis to the pluviographic and pluviometric data in order to define a specific rainfall event to be modelled. The frequency analysis was also developed to define design hyetographs for 50 and 100 years return period based on intensities for different duration and return periods. Three infiltration methods were considered to assess its effect on the total precipitation. The third stage consists in the DEM processing using three different DEM sources. This stage defines the catchment geomorphological parameters, the Strahler's stream ordering map and the Horton's statistics parameters. These three stages become the basic input for the GIUH modelling. The GIUH showed a reasonable model efficiency of 67% and its instantaneous unit hydrograph from this simulation was used to estimate the design discharge values for 50 and 100 years return period. These discharge values become a good reference for hydraulic structures design projects especially those developed at the bottom part of the catchment, where the urban area is located. The variation among the Horton's statistics values estimated for every DEM source did not affect significantly the peak values of the unit hydrograph. This performance suggests that the use of a free access satellite imagery source such as the SRTM can perform successfully and efficiently with the GIUH model.

Keywords: SRTM, GIUH, Frequency analysis, DEM hydro-processing

Acknowledgements

First of all I would like to thank the International Institute for Geo-information Science and Earth Observation (ITC) for providing me the academic and financial support to pursue my Master program study.

I want to express my gratefulness to CLAS-UMSS in Cochabamba - Bolivia, for their help to obtain the scholarship, and receiving the opportunity to study for a master degree in a foreign country such as The Netherlands.

I would also like to express my sincere gratitude to all the ITC staff, for their permanent support and advice. My special gratitude to my supervisors MSc. Ir. Gabriel Parodi and Dr. Dinand Alkema for their knowledge, suggestions and help provided throughout my study period and thesis time which have helped me to a great extent.

My sincere gratitude to the Department of Agricultural and Food Engineering, of the Indian Institute of Technology, Kharagpur for their help with the GIUH methodology.

I am grateful to the Watershed Management Division of the Municipal Government of La Paz City for providing me the data necessary for this study, and to all the friends and colleagues who shared discussions and suggestions with me.

I would like to express my special gratitude to all my family, my mother Esthela, my father Angel, my sister Gelsy and my brother Adhemar, who have been supplying me with moral support, love and motivation during my whole study period.

My stay in the Netherlands wouldn't have been so pleasant without all the new friends I met here, all the good moments and the nice experience of sharing with different cultures. My gratitude to all of them, especially to my country mates, Nelson, Carlos, Luis and Juan Pablo.

Finally, I wish to forward my appreciation and thankfulness to her, who is always by my side to turn off my loneliness, who gives me the strength, the courage and reality to feel a little alive… more than for me is for her for whom I live… she is the music…

Table of contents

List of figures

List of tables

1. Introduction

Estimation of the time-response characteristics of a catchment is fundamental in hydrologic analysis and rainfall-runoff response modelling, mainly in basins leading to urban areas. Responses to real or design rainfall, such as peak discharge, hydrograph recession, and the time evolution of cumulative runoff, are greatly influenced by time characteristics. Rainfall-runoff models that incorporate timing parameter variables are used by engineers and others for hydrologic design purposes, including the design of bridges, culverts, and detention facilities. (Cleveland et al., 2007).

Catchment models are in general designed to gain a better understanding of the hydrologic behaviour of a catchment and the influence of changes in the catchment. A secondary goal of catchment modelling is the generation of synthetic hydrologic data to facilitate the design like water resources planning, flood protection, mitigation of contamination, or licensing of abstraction or for forecasting. They are also providing valuable information for studying the potential impacts of changes in land use or climate. (Nguyen Hong, 2006)

One of the most important steps toward hydrology analysis and construction of the hydrographs for a given project is the development of Unit Hydrograph concept. A Unit Hydrograph is by definition, a hydrograph having a volume of 1 mm of runoff which is associated with a precipitation event of specified duration and areal pattern (uniform over the basin) The special thing about the Unit Hydrograph is that it enables us to derive the Hydrograph of flood design, based on which the hydraulic structure is to be designed. (Noorbakhsh et al., 2005).

The geomorphological theory of the unit hydrograph has been formulated by Rodriguez-Iturbe and Valdés (1979). This model is called GIUH (Geomorphological Instantaneous Unit Hydrograph), and provides the times of transfer according to the geomorphology of the drainage basin. (Fleurant et al., 2006). GIUH’s proposed to estimate floods for ungauged streams by using only the information obtainable from topographic maps or remote sensing possibly linked with the Geographic Information Systems (GIS) and Digital Elevation Model (DEM). (Shaheen et al., 2005). Among last investigations made to this model, we can mention Bhadra et. al. (2008) who developed a user-friendly event based computerized GIUH model, the GIUH_CAL, which is going to be used for this study.

1.1. Research problem

The use of conventional and well known rainfall-runoff methods requires available and specific field data. Precipitation, run-off, soil characteristics, etc. are some examples of these variables. In order to get and monitor these parameters catchment instrumentation is required.

Adequate run-off data, field information and meteorological station instruments are generally not available for small and medium size catchments, particularly in developing countries like Bolivia.

During the rainy period (November to March) the capital city of Bolivia, La Paz, is vulnerable to overflows and flooding due the high slope, variable topography of the surrounding area, old sewerage system and human settlements across the riverside and hill slopes established against safety regulations.

On February 19th 2002, a convective cell travelling from North to South, caused precipitation with electric storms and high intensity hailstorms, exceeding the historical record dated from 1940. A maximum intensity, registered at the Laycakota Meteorological Observatory, had a total volume of 34 mm in 50 minutes [41 mm/h].

The Meteorology and Hydrological National Service (SENAMHI), does not have a modern communication system. The lack of this technology limits engineers for having a better forecast. Adequate meteorological instruments also become important in order to assess these kinds of storms and develop an optimal early alert system.

This extreme rainfall event showed the fragile vulnerability of the city to heavy storms. According to the press and governmental reports most of the hydraulic structures failed or collapsed due the runoff generated. The total amount of damage was estimated in 10 million U$S, 63 people died, 144 were harmed and 13 missing. It was also demonstrated that the hydrological network is insufficient in density and quality. The upstream area of the catchment has no instrumentation, which implies a total ignorance related to its hydrological behaviour.

Accurate estimation of surface runoff from rainfall events over watersheds has been attempted by researchers through the use of different empirical, conceptual and physics-based approaches. Amongst all the techniques, the unit hydrograph (UH) method widely used for rainfall runoff analysis for ungauged watersheds. (Sarangi et al., 2008).

Due to non-existent instrumentation in the catchment the implementation of the GIUH methodology will become potentially a powerful tool to estimate the runoff generated. Urban planning and water management programs will be developed with much more accuracy supported on a reasonable understanding of the catchment hydrology.

1.2. Objectives

The main objective of this thesis is to develop the GIUH to assess its performance for the Achumani catchment for the city of La Paz, Bolivia.

The specific objectives are:

- To assess the applicability of GIS and RS techniques as a tool for data collection applied to GIUH developments.
- To assess the influence of the DEM source for the geomorphology parameters.
- Estimate design runoff values for hydraulic structures for return periods of 50 and 100 years.

1.3. Research questions

- Can GIS and RS techniques be considered accurate tools for data collection, particularly for geomorphological parameters of a catchment?
- How do the DEM source and its assessment affect the GIUH performance for the Achumani catchment?
- Is it possible to make an accurate frequency analysis for ungauged catchments based on the existing data?

1.4. Hypothesis

The development of the GIUH methodology will derive in a hydrograph with reasonable accuracy, compared to the previous studies and calculations made on the runoff for the study area.

The GIUH procedure presented in this study can be implemented in other ungauged sub catchment of the surrounding target area.

2. Study area

2.1. Geographic location

La Paz department is located in the northwest part of Bolivia. It has an area of 133,985 Km^2. Its capital is the city of La Paz, which as well is the central government capital of Bolivia. La Paz is located at 3640 m.a.s.l. Its boundaries are: to the north with Pando, to the south with Oruro, to the east with Beni and Cochabamba and to the west with Perú and Chile.

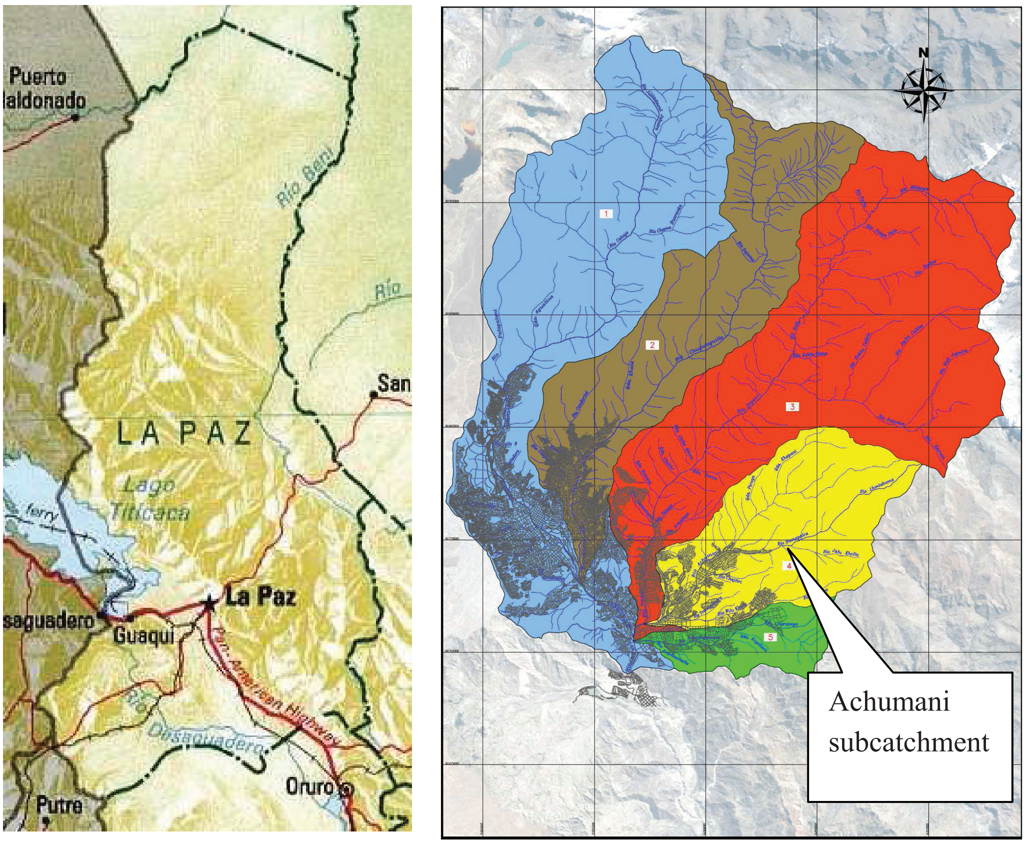

Figure 1 La Paz department. Southwest of Bolivia (left) Achumani catchment (right) (PCA Consulting Engineers and NIPPON KOEI CO. LTD., 2007)

It is located between 16°30'00"S and 68°08'00"W. The department of La Paz has approximately 1.484.328 habitants. It is divided into 20 provinces and 272 cantons.

2.2. Catchment description

The La Paz river is part of the macro Amazonas catchment. It represents the headwaters of the Boopi river, the main tributary of the Beni River, which after converging with Madre de Dios, Mamoré and Itenez rivers originate the Madera river. The La Paz river catchment consists of five sub catchments, Choqueyapu, Orkojahuira, Irpavi, Achumani and Huayñajahuira. This river crosses the city and has around 230 affluent rivers and creeks. The present study will be developed in the Achumani catchment, (See Figure 1).

2.2.1. Topography

The La Paz catchment area is approximately 495.1 km^2; the longest stream length is 37 km. Its altitude varies from 5300 m.a.s.l. in the upstream area to 3125 m.a.s.l. at the outlet. Figure 1 shows the Department of La Paz and the La Paz catchment with its five sub catchments.

The catchment topography is abrupt. The upper and medium stream areas present high slope and deep gullies product of the precipitation in soils with low cohesion. The lower part of the catchment consists of areas of low slope where continuous problems of material deposition are present.

2.2.2. Precipitation

The annual precipitation for the different pluviometric stations is between 500 and 600 mm. The catchment precipitations have a seasonal behaviour; the maximum precipitations are registered in the wet period, from November to March. Approximately 77% of the annual precipitation is recorded in this period, the 17% is registered in April, September and October whereas during the dry period is 6% only.

2.2.3. Achumani sub catchment

The Achumani river is born at the Chachacomani hills, which has altitudes higher than 4944 m.a.s.l. The flow direction is southwest.

Figure 2 shows the Achumani catchment, which area is approximately 62 km^2. Its principal stream length is around 15.7 km..

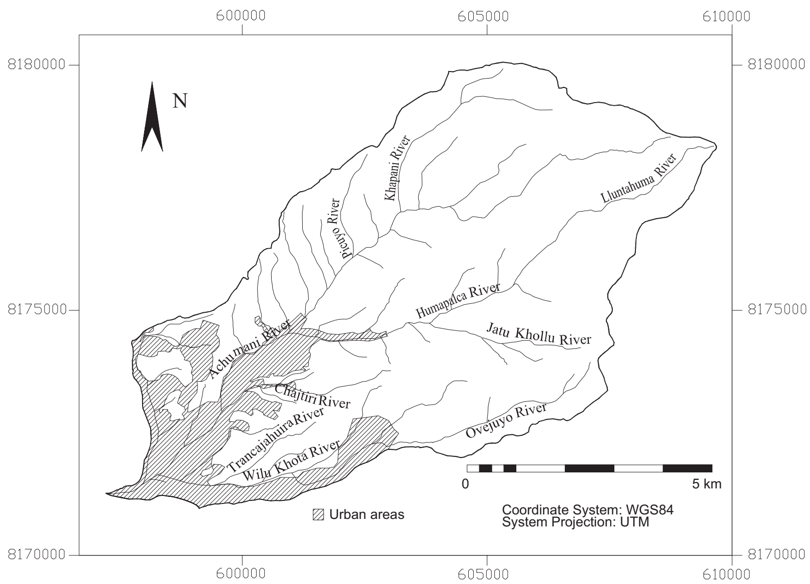

Figure 2 The Achumani catchment

The longitudinal slope of the stream is high in the upper part of the catchment. During the rainy period, due to its abrupt slope, precipitation causes high erosion indexes, and as a consequence sediment blocks the outlets. Slope profile can be observed in Figure 3

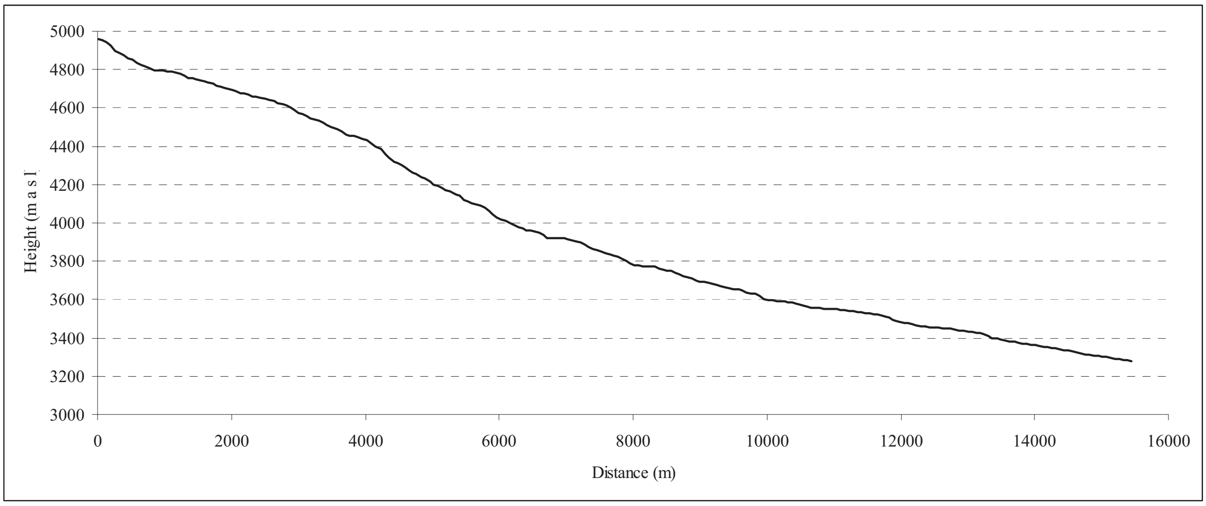

Figure 3 Longitudinal profile of the Achumani river

2.2.4. Geology and geomorphology

The geomorphological processes get an especial relevance due to the geological configuration of the La Paz catchment. They are conformed by soils with different degree of consolidation (approximately 60%) and by rock from different geological ages (40%).

The city is built entirely over soil; this makes it highly vulnerable to pluvial erosion, including precipitation over vertical soil walls in the hillsides and creeks in the five sub catchments and the runoff over natural slope.

The Huaripampa and the Wila Pampa plain, located at the headwaters of the Kellumani river are conformed by moraines and fluvioglacis material.

This type of relief suffered a dissection process with de valley glaciation, forming in this way the glacial valleys in the higher drainages of the Choqueyapu, Orkojahuira and Irpavi river, where these lateral and frontal moraines were deposited along its stream. This erosive phenomenon can be clearly appreciated in aerial photographs and satellite imagery.

The Achumani and Huayñajahuira rivers start as slope streams due to the precipitation and the groundwater contribution, finding downstream soft and erodible terrains.

The lower part of the Achumani and Irpavi rivers, have developed a more mature erosion cycle, locating it below its natural balance level. At this stage lateral scour, sediment accumulation, produce an elevation of the river bed due the heavy material that can not be carried by the water. Due to these characteristics these two rivers are considered under-fit.

The La Paz catchment is settled over the La Paz formation, which is located over a rock bed. The La Paz formation is conformed by sand, clay and silt in its lower part and gravel layers interbedded in the upper horizon, and a horizon of volcanic ashes in the top of the formation. The different erosion problems have modelled the surface and defined deep valleys, hillsides and steep interflows.

3. Research methods

3.1. Methodology

In order to develop the GIUH methodology, three stages were defined.

- Pre fieldwork
- Fieldwork
- Post fieldwork

3.1.1. Pre fieldwork

This stage is related to the basic activities needed to the overall understanding of the GIUH methodology. These activities include:

- Bibliographic review (ITC library, Elsevier, Web of Science, Water Resources Research, etc.)
- Satellite images for land cover classification and DEM processing studies over the study area (Landsat, Quickbird)
- Available data for the study area (Hydrology, topography, discharge measurements, previous studies made in the area). This activity is important because according to available data, a specific rainfall event will be chosen for the modelling process.

3.1.2. Field work

Three different activities were carried out during the fieldwork period: data collection, field measurement and field survey.

- Data collection

Type of Data	Source	Detail
Geographic sheets	Geographic Military Institute (IGM)	Scale 1:50.000 Contour levels every 20 m
Detailed channel network and profile at the outlet of the catchment.	Municipal Government of La Paz city	Local studies developed for structures design purposes
Discharge measurements	Municipal Government of La Paz city	Period 1989-1993 (Automatic Limnigraph)
Hydrological Information (Rainfall data)	Meteorological and Hydrological National Institute (SENAMHI)	Millipunku station (1987-2000) (pluviometer) Millipunku station (1991-1994) (pluviograph)
Infiltration data	PCA Consulting Engineers	Field Measurement of Infiltration Rate Using Double-Ring Infiltrometer
Previous studies made in the area	Municipal Government of La Paz city, San Andres Major University UMSA, Hydraulic and Hydrology Institute IHH	Hydraulic Structures design Hydrological estimations Thesis developed in the area

Type of Data	Source	Detail
Satellite Imagery	Geographic Military Institute (IGM)	Landsat (June, 2002) image for georeferencing purposes
Digital aerial orthophotos	Municipal Government of La Paz city	2006 Aerial photos

Table 1 Detail of the data requirements for the study

- Field measurement

As mentioned earlier, the rainy period in the La Paz catchment and its five sub catchments is from November to March. However, the channel network was inspected in order to find water marks product of storms during the last rainy periods. This information needs an additional topographic data, since a reasonable number of cross sections and longitudinal profile are needed to estimate the water discharge. Thus, the topographical survey was part of the fieldwork. Figure 4 shows part of the field measurements made during the fieldwork period. Different cross sections were measured for calibration purposes (left), water marks found inside the channel system at the outlet of the catchment (center) and along the natural stream in the medium part of the catchment (right).

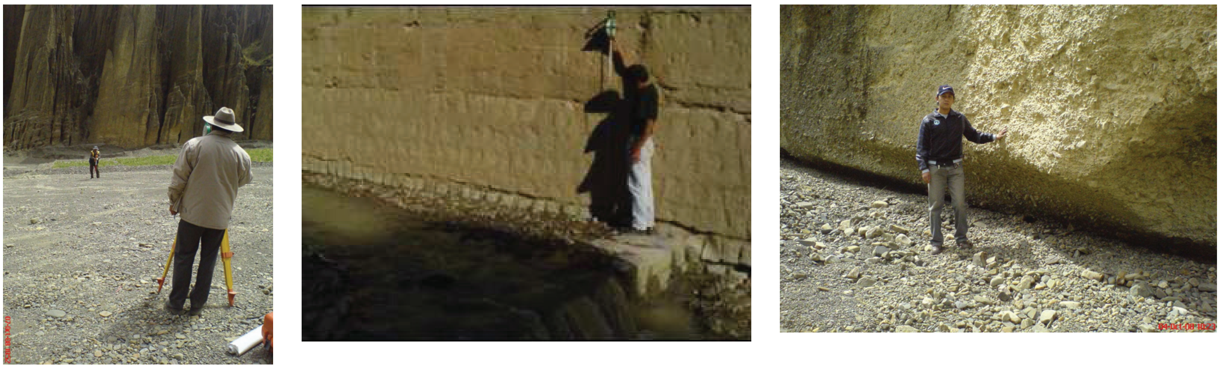

Figure 4 Field measurements activities during the field work period

- Field survey

Ground control points collection was made in order to determine an accurate drainage network, which becomes the main input data for the geomorphological parameters analysis The GCP shown in Figure 5, belong to the outlet of every important stream that drains into the principal stream.

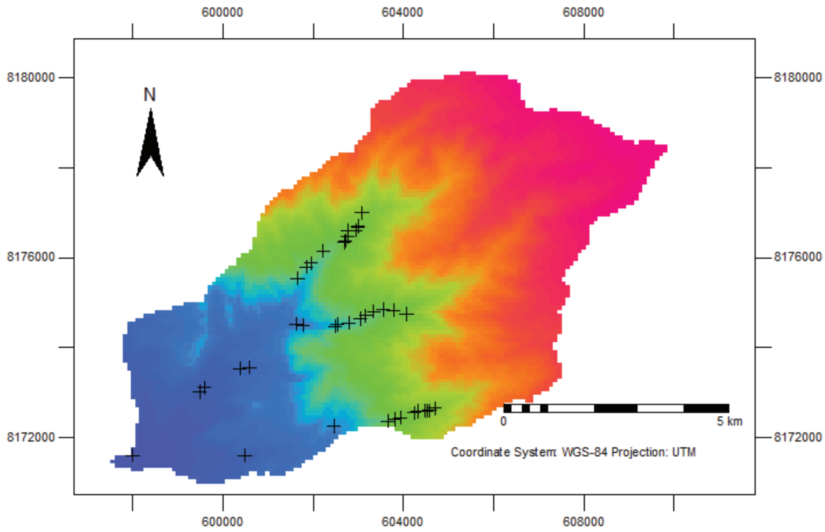

Figure 5 GPS Ground Control Points collected for the drainage system definition

Visual inspection was made in order to define the type of vegetation and land use in the surrounding area for the elaboration of the land cover and use map.

3.1.3. Post fieldwork

3.1.3.1. Remote sensing and GIS

- Land cover classification (Supervised method))
- DEM processing using three different sources: SRTM imagery, topographic maps and Aerial orthophotos restitution.
- Determination of drainage network and catchment delineation (Figure 6)
- Determination of the geomorphological characteristics of the Achumani catchment, the Strahler stream order and the Horton's statistics parameters.

Figure 6 shows the flowchart for the determination of the catchment delineation and geomorphological parameters definition.

The first line of the flowchart defines the Flow Determination, a set of routines that facilitates the necessary pre-processing steps to derive a hydrological consistent flow network. The main processes at this stage are:

- The Fill Sink operation which removes local depressions (of single pixels and of multiple pixels) from the DEM.
- The Flow direction operation determines into which neighbouring pixel any water in a central pixel will flow
- The Flow accumulation which performs a cumulative count of the number of pixels that naturally drain into outlets.

The next stage for the catchment delineation consists in the Network and Catchment Extraction. This stage includes 4 subroutines:

- The Drainage Network Extraction operation which extracts a basic drainage network (boolean raster map),
- The Drainage network ordering operation finds individual streams within a drainage network and assigns a unique ID to each stream,
- The Catchment extraction operation constructs catchments for each stream found in the Drainage network ordering map.
- The Catchment merge operation which merges adjacent catchments.

Additionally to the operations explained above, is the Statistical Parameters extraction module. In this module, a number of functions are given to provide relevant statistical information of the extracted river and catchment network.

The Horton plots show the relationship between Strahler order and total number of Strahler order stream segments for a given order, average length per Strahler order and average catchment area per Strahler order, as well as the bifurcation, channel length and stream area ratio’s (Maathuis B.H.P. and Wang L., 2006) (Further explanation will be developed in Section 3.2.1)

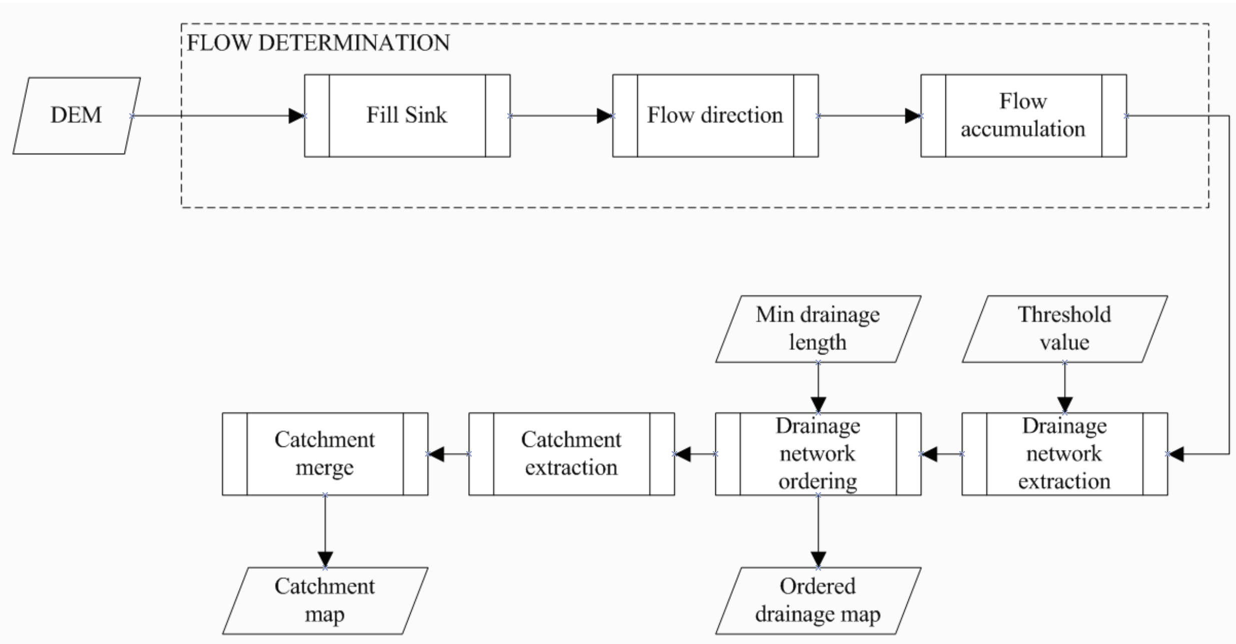

Figure 6 DEM processing steps to extract the drainage network and catchment

3.1.3.2. Hydrology analysis

During this stage, all the pluviographic and discharge measurements data collected in the fieldwork will be organized and presented in final graphics for its interpretation. According to the information available, a single event will be used to develop the GIUH methodology.

The frequency analysis for the Millipunku station will be made to get the Intensity – Duration – Frequency [IDF] curves to define the design hyetograph for 50 and 100 years return period. The criteria used to select these return periods is based on the Bolivian Normative NB 688, which suggests the following return periods for drainage system design.

Return Period (years)	Type of structure
1 – 2	Urban and sub urban areas network
2 – 5	Urban, residential and commercial areas network
20 – 30	Principal and secondary collectors
30 – 50	Collectors, interceptors and emissaries
100	Catchment global drainage system

Table 2 Return period for drainage system design

In order to consider the infiltration processes that affect the total precipitation over the Achumani catchment, three infiltration methods were selected for evaluation to determine the effective rainfall. The methods adjust to the condition of data scarcity.

- The SCS effective rainfall method based on the initial abstraction
- The Phi-index method
- The Kostiakov model

3.1.3.3. GIUH modelling

This stage of the study includes:

- GIUH modelling, using the GIUH_CAL software (Bhadra et al., 2008)
- Sensitivity analysis using the Horton ratios values.
- Calibration based on the Mean holding time [K_B], calculating it from rainfall-runoff data set.
- Performance indicator analysis using an error function method based on the difference between observed and computed peak discharges presented by Nash and Sutcliffe (1970).
- Frequency analysis to estimate discharge values for 50 and 100 years of return period, as needed for structural design.

Additionally to the calibration process and considering the cross sections and the water marks obtained during the field work, the water discharge generated during a big storm will be estimated. The estimated discharge value will become criteria to evaluate the results from the GIUH model.

3.2. Literature review

3.2.1. Geomorphological Instantaneous Unit Hydrograph (GIUH) model

The geomorphological instantaneous unit hydrograph (GIUH) model is based on the theory proposed by Rodriguez-Iturbe and Valdes (1979).

The main purpose of this method is to relate the geomorphological characteristics of a catchment to its response to rainfall. The Strahler stream order (Strahler, 1957) and the Horton's morphometric parameters are mainly used to develop this theory).

The Horton Statistics operation calculates for each (Strahler) stream order number and for each merged catchment the area ratio (R_A), bifurcation ratio (R_B), and length ratio (R_L).`

Bifurcation	$R_B = \frac{N_i}{N_{i+1}}$	where N_i and N_{i+1} represent the number of streams in order i and i+1. Let ω

		represent the highest stream order in watershed, i = 1, 2,…, Ω
Length	$R_L = \frac{L_{i+1}}{L_i}$	Li is the average length of channels of order i $L_i = \frac{1}{N_i}\sum_{j=1}^{N_i} L_j$
Area	$R_A = \frac{A_{i+1}}{A_i}$	A_i is the mean area of the contributing subcatchment to streams of order i, $A_i = \frac{1}{N_i}\sum_{j=1}^{N_i} A_j$ where A_j represents the total area that drains into the jth stream of order i

Table 3 Horton statistics parameters

These ratios are obtained using a least square fit through (logarithm transform) points of e.g. the number of stream per order. The ratio value represents the increase or decrease in number, length and area from one order to the next. (Maathuis B.H.P. and Wang L., 2006)

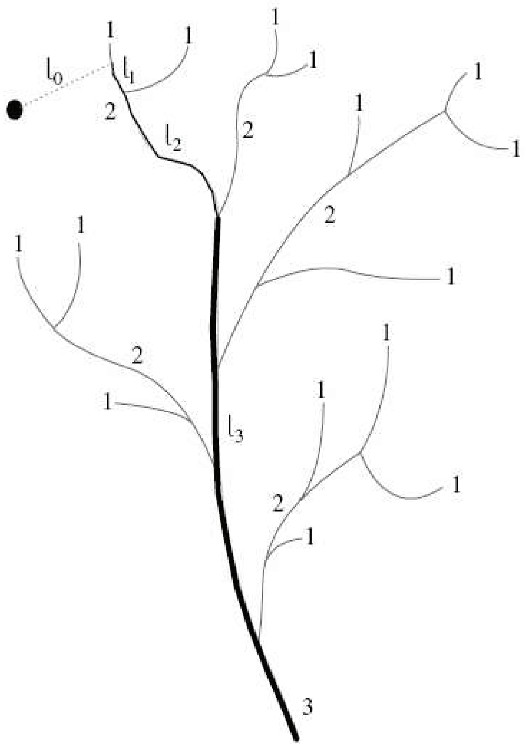

Figure 7 Strahler's stream order classification (Fleurant et al., 2006)

Figure 7 shows a hypothetical watershed with the Strahler ordering procedure:

1) Channels that originate at a source are defined to be first-order streams

2) When two streams of order w join, a stream of order Ω + 1 is created

3) When two stream of different order join, the channel segment immediately downstream has the higher of the order of the two combining streams.(Rodriguez-Iturbe and Valdes, 1979).

This original formulation of GIUH is based upon the probability density function (pdf) of the time history of a randomly chosen drop of effective rainfall arrived to the outlet of a hypothetical catchment treated as a continuous Markovian process. (Kumar et al., 2007). Using more specialized methods Gupta et. al. (1980) obtained a different expression. The instantaneous unit hydrograph model proposed, is developed to establish the instantaneous unit hydrograph (IUH) ordinate, h(t), for the watershed using the following equation:

$$h(t) = \sum_{s\in S}\sum_{j=1}^{k} C_{jk}\exp\{-\lambda_{xj}t\}p(s) \quad \textbf{Eq. 1}$$

$$C_{jk} = \frac{\lambda_{x1}\lambda_{x2}\ldots\lambda_{xk}}{(\lambda_{x_1}-\lambda_{x_j})(\lambda_{x_2}-\lambda_{x_j})\ldots(\lambda_{x_{j-1}}-\lambda_{x_j})(\lambda_{x_{j+1}}-\lambda_{x_j})\ldots(\lambda_{x_k}-\lambda_{x_j})} \quad \textbf{Eq. 2}$$

Where:

S is the set of all possible paths

p(s) is the path probability

C_{jk} is the coefficient (probability density function proposed by Feller (1971)

λ_x is the parameter (dependent on mean holding time of the basin)

k is the number of states in a particular path, s is the path index, j is the state index, and t is the time. (Bhadra et al., 2008)

To estimate the coefficients, C_{jk}, the mean holding time of a ith-order Strahler's channel $1/\lambda_{ci}$ and mean holding time of a ith-order overland region $1/\lambda_{ri}$, are assumed to be proportional to some characteristic length. This assumption is necessary to estimate C_{jk} (Gupta et al., 1980)

$$\frac{1}{\lambda_{c_i}} = \gamma \overline{L}^{1/3} \quad 1 \le i \le \Omega \quad \textbf{Eq. 3}$$

$$\frac{1}{\lambda_{r_i}} = \gamma \left[\frac{\pi_{r_i} A_\Omega}{2 N_i L_i} \right]^{1/3} \quad 1 \le i \le \Omega \quad \textbf{Eq. 4}$$

Where:

γ is the proportionality factor

Li is the mean length of channels of order i,

Ω is the order of basin

π_{ri} is the initial state probability

A_Ω is the area of basin of order Ω

N_i is the number of channels of order i.

Proportionality factor, γ, is estimated from the mean holding time of the basin, K_B, which is equal to the distance (measured in time) between the centre of gravity of the observed hydrograph and the centre of gravity of the observed hyetograph.

The probability of a drop taking a path $s \in S$ of the form $s = \{x_1 \ldots x_k\}$ where $x_i \in \{r_1, r_2, \ldots, r_\Omega, c_1, c_2, \ldots, c_\Omega\}$ is given as follows:

$$p(s) = \pi_{x_1} p_{x_1,x_2} \ldots p_{x_{k-1},x_k} \quad \textbf{Eq. 5}$$

Where:

π_{xi} is the initial state probability (the ratio of the area r_i to the total area of the basin)

$p_{xi\,;xj}$ is the transitional probability (the ratio of the channels of order i falling into channels of order j to the total number of channels of order i), and i and j are the order indices.

According to the formulation proposed by Gupta (1980) the symbol c_i is used to denote a channel state of Strahler order i (an ensemble of all the channels of order i). Similarly, r_i denotes an overland region state of Strahler order i (an ensemble of the overall flow areas and/or creeks smaller than the first-order channel which flow directly into the channel of order i).

The model subsequently estimates the direct runoff hydrograph (DRH) ordinate for different sets of rainfall data by convolution of small duration effective rainfall and IUH using following equation:

$$Q(t) = \int_0^{t'} h(t-\tau)I(\tau)d\tau, \quad t' = t \quad when \quad t < t_0 \qquad \textbf{Eq. 6}$$
$$t' = t_0 \quad when \quad t \geq t_0$$

Where h(t) is the IUH ordinate and I(τ) is the effective rainfall of t_0 duration.

Further explanation of the GIUH methodology is made in Appendix 2. Additionally, an example is developed using this methodology.

3.2.2. The GIUH_CAL model

Bhadra et. al. (2008) developed a user-friendly event based computerized GIUH model, GIUH_CAL. The model algorithm is based on the formulation described in Section 3.2.1.

Additionally the model offers a choice among three methods of infiltration calculation: Richards' equation, phi-index method and Philip two term model, which may not be needed in case the work is done considering effective rainfall

Figure 8 shows a flow diagram of the GIUH_CAL model. Two major modules can be observed, MAIN and INFILTRA. The MAIN module works based on the vector information product of GIS techniques (DEM processing, catchment definition, drainage network order and Horton's statistics parameters). Using these pre-processed geomorphological data, the MAIN module estimates initial state and transition probabilities as well as path probabilities. INFILTRA module is then executed to estimate the net effective hyetograph for the supplied set of input (rainfall data). Using the observed direct runoff hydrograph and the estimated net effective hyetograph, the mean holding time, K_B, of the basin is estimated, and subsequently used to estimate the proportionality factor γ. The λ_{xk} values are then estimated from γ and geomorphological features, whereas C_{jk} values for each path are estimated from λ_{xk} values. Finally, instantaneous unit hydrograph ordinate, h(t), is estimated from the C_{ij} and p(s) values, as well as direct runoff hydrograph ordinate is calculated from h(t). (Bhadra et al., 2008)

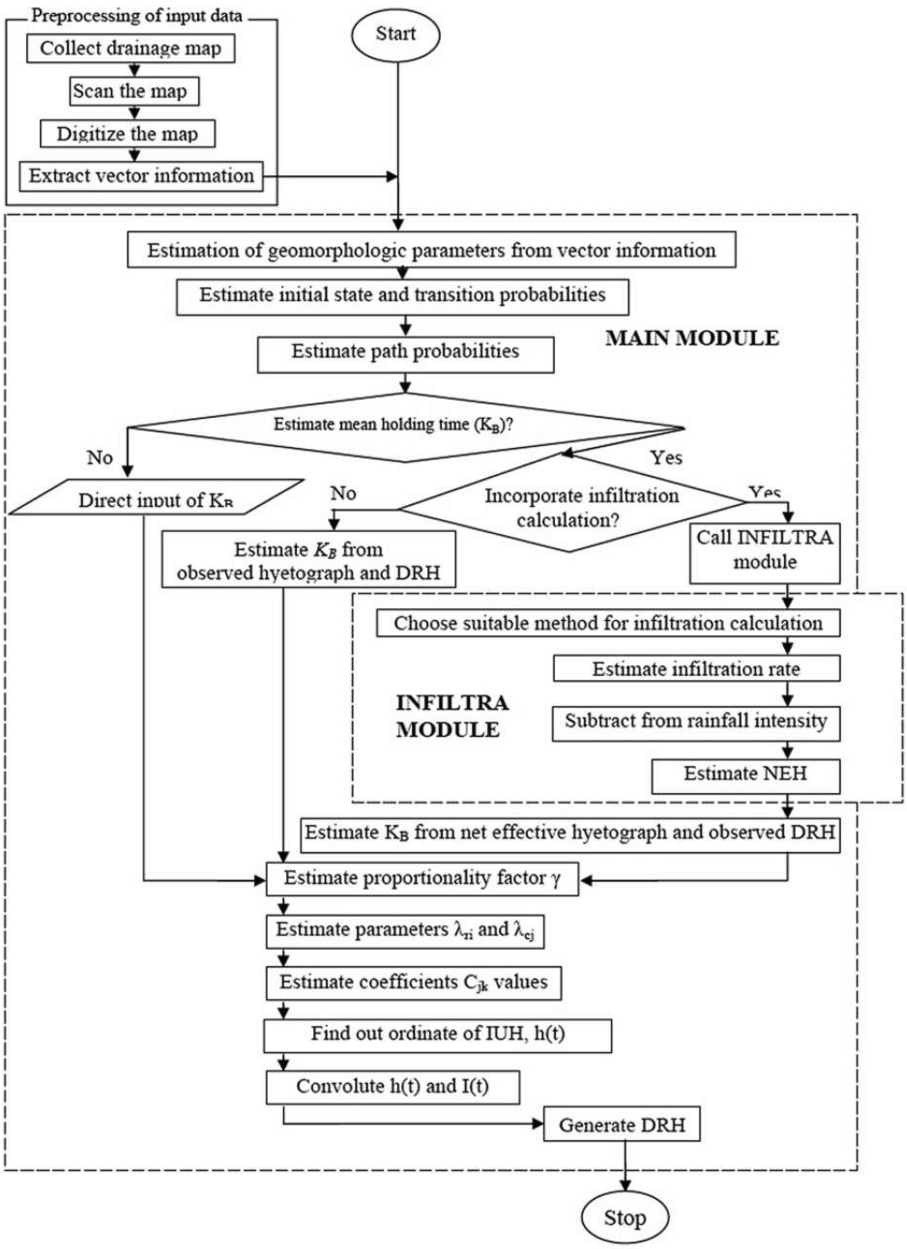

Figure 8 Flowchart of the GIUH_CAL model (Bhadra et al., 2008)

3.2.3. Input data requirement

The main input data for the GIUH modelling are:

- Rainfall Information,
- Runoff Information
- Geomorphological Information
- Infiltration Information

For the estimation of the geomorphological parameters, the drainage network ordering map needs to be processed according to the flowchart presented in Section 3.1.3.1.

3.2.4. Output information

Different hydrographs are generated.

- IUH (Instantaneous Unit Hydrograph) or DRH (Direct Runoff Hydrograph) are generated by specifying Tmax (maximum base period) and Interval for the ordinates.
- UH (Unit Hydrograph) is generated specifying the duration of the rainfall in addition to the other two data.

Additionally the model presents statistical performance criteria which are used for estimating the quantitative performance of the GIUH_CAL model. The performance indicators used are:

- Modelling efficiency
- Root mean square error
- Coefficient of determination

3.2.5. Previous studies developed using the GIUH approach

Many studies were developed using the GIUH and it has been demonstrated its suitability to different environments. Shaheen (2005) developed an application of the unit hydrograph theory and the GIUH to semiarid regions. Shadeed (2007) modeled the rainfall-runoff process in Faria catchment located in the northeastern part of West Bank, Palestine. The influence of land use on catchment runoff was modeled by Karvonen (1999) and it was made using the GIUH. Nguyen (2006) developed the GIUH methodology for an ungauged catchment in the Sigon river. Jain (2003) used the GIUH model for a 5th order stream in the Himalayan river, deriving with it the first ever analytical UH of the river

For further information related to the methodology, refer to Gupta et. al (1980) and Bhadra et. al. (2008)

4. Data analysis and preparation

4.1. Hydrology

As it was mentioned in Section 3.1.2, two main types of hydrological information were collected: the pluviograph information from Millipunku station (1991-1994) and the discharge measurements from the automatic limnigraph (1989-1993). Figure 9 shows the location for both stations.

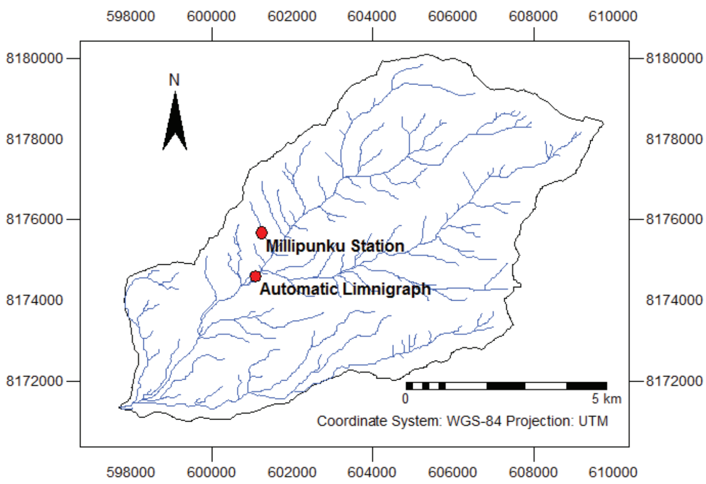

Figure 9 Spatial location for rainfall and runoff data collection

Much effort was made to organize all this information. Unfortunately most part of the original information from the pluviograph was lost and the only available information consists in the printed reports. Relative to the limnigraph information, the original file from the equipment was found, but as it was made during the 80's, an ASCII file ordered by rows and columns was all the information. Fortunately this file contained the waterlevel-discharge transformation using a rating curve. Much time was invested making a reasonable data base and graphical data for this study.

From the rainfall data analysis made to the record period, there are only four considerable months with precipitation above 15 mm/day (Dec-1990, Jan-1991, Dec-1991 and Jan-1992). Combining this data with the discharge records, the resulting graphs for Dec-1990 and Dec-1991 are presented in Figure 10 and Figure 11.

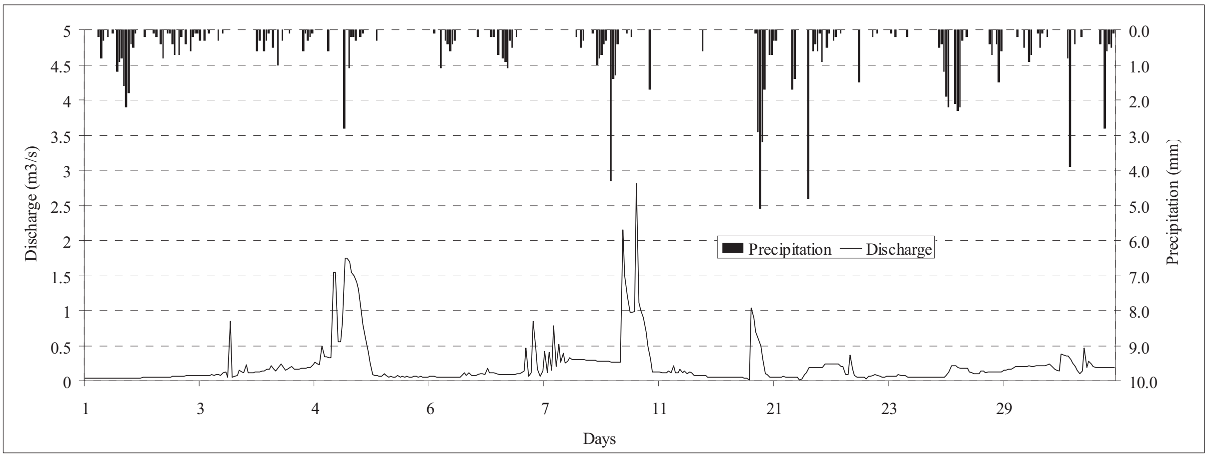

Figure 10 Precipitation and discharge graphs for Dec-1990

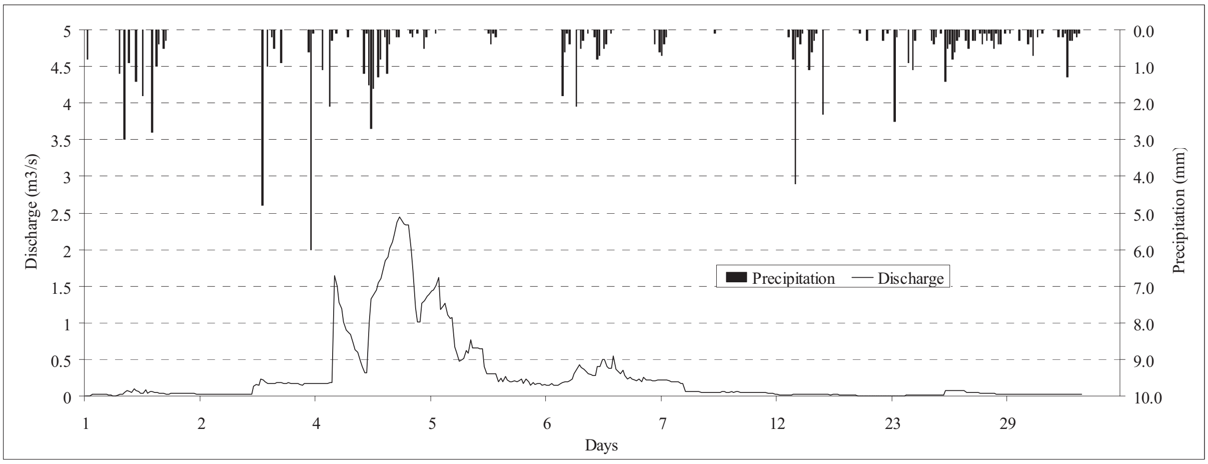

Figure 11 Precipitation and discharge graphs for Dec-1991

From Figure 10 it can be observed that the catchment does not have a normal response to runoff generation. It is expected to have a time of concentration of around 3 hrs (PCA Consulting Engineers and NIPPON KOEI CO. LTD., 2007) but in this case it is necessary two or three days of precipitation. See the first two days of precipitation with low discharge response and at the 3rd day a more reasonable amount of discharge. Something similar happens during day 20th. There might be two possible explanations to this characteristic: The type of rain and the type of soil.

The type of rain over the La Paz is characterized for its spatial variability. During extreme events (>30 mm/day), the south part of the city (where the Achumani catchment is located) presents high intensity and short duration rainfall. This spatial variability can explain that a local precipitation was registered in the station; meanwhile the rest of the catchment was dry, generating low discharge response.

The type of soil over the Achumani catchment presents high erosion indexes. According to the soil map developed by the Remote Sensing Application and Research Center CIASER-GEOBOL (1985) (For further information refer to PCA(2007)) the soil type classification is as follows.

C.1.6.1 Soils with steep to high steep slopes. Moderately deep to deep. Highly erosive with gullies. Loam, sandy clay loam, silt clay loam, silt loam Low to moderate nutrient content with outcrops.

This type of soil could explain the three-day precipitation with low runoff generation. During this period, if the rainfall intensity at the soil surface occurs at a rate that exceeds the infiltration capacity, ponding begins and is followed by runoff over the ground surface, once depression storage is filled.

Based on the infiltration measurements made by PCA, the Achumani catchment has infiltration rates of around 108.8 mm/hour which belongs to a moderately fast infiltration rate (Porta J. et al., 1999). From this study, the conclusion is that the infiltration volume will be higher than the runoff during a storm intensity that exceeds the basic infiltration velocity.

Considering this characteristic, 4-December-1991 provides a good rainfall event to be modelled, because during the previous three or four days there was enough precipitation to saturate the soil. Figure 12 provides a good view of this event. One important assumption for the modelling process is to consider this event as uniformly distributed over the catchment area. Unfortunately the lack of information and having only one station (out of work since 2002) are the principal reasons for this.

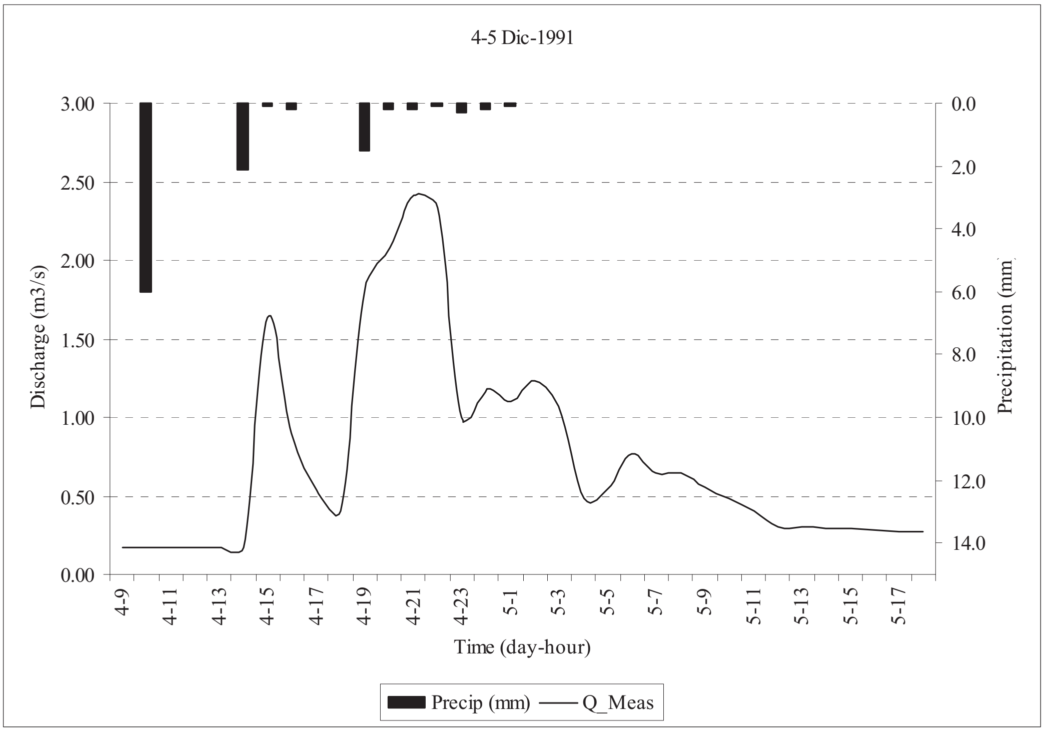

Figure 12 Precipitation and discharge for December 4th, 5th 1991

4.2. Frequency analysis

One of the specific objectives in this thesis is to determine design discharge values for different return periods (50 and 100 years). In order to estimate these values using the GIUH methodology, it is necessary to obtain the Intensity – Duration - Frequency curves to define the final design hyetograph for the two return periods considered.

As it was mentioned before, the record period for the Millipunku station (pluviographic information) is from 1990 to 1994. Unfortunately this record period is too short to define a reliable frequency analysis. However, the results obtained from this analysis will be compared to the design hyetograph using distribution coefficients defined by Mendoza (2000). In this study, the San Calixto meteorological station, which becomes the only station with record periods over 40 years, was used.

The first step consists in defining maximum precipitation values for different time periods based on the pluviographic information that was collected during the fieldwork. 24 events were selected and they are presented in Table 4.

	Duration in minutes									
Date	15	20	30	45	60	120	180	360	720	1440
8-Jun-90	1.50	2.30	3.00	4.20	7.20	11.50	14.10	14.90	20.40	36.90
26-Sep-90	2.10	2.80	3.50	4.80	9.40	16.30	19.70	23.50	23.50	23.90
31-Dec-90	8.20	10.90	12.70	14.00	15.40	16.00	16.40	16.90	18.40	22.80
25-Jan-91	6.50	8.20	8.50	9.10	9.80	13.70	14.30	16.90	17.30	28.10
12-Aug-91	6.20	7.70	7.90	8.10	11.00	18.30	19.50	19.60	19.60	29.50
13-Mar-91	1.90	2.70	3.00	3.80	7.20	12.00	14.30	19.00	21.80	22.30
2-Nov-91	2.10	3.00	3.80	5.60	8.70	14.90	18.90	21.40	23.40	24.40
26-Nov-91	1.80	2.10	2.40	2.90	5.30	6.60	7.00	9.70	15.00	20.20
4-Dec-91	2.90	4.30	5.60	7.70	11.00	14.00	14.70	17.30	22.20	32.70
6-Jan-92	2.90	4.40	5.00	6.20	6.80	9.50	10.70	11.20	13.30	23.30
15-Jan-92	1.50	2.30	3.00	4.40	6.60	7.10	7.70	8.50	12.80	20.30
14-Feb-92	3.30	4.90	6.60	8.50	10.00	13.60	14.10	14.10	19.20	19.40
22-Nov-92	2.70	3.60	4.60	6.50	11.40	15.60	17.00	18.10	28.70	48.10
7-Dec-92	3.20	4.20	5.00	7.60	10.20	15.00	17.80	24.20	26.10	29.40
10-Jan-93	4.10	6.10	8.20	11.80	22.20	28.30	29.30	29.30	29.30	29.30
19-Jan-93	4.70	7.10	8.50	11.40	15.10	16.80	16.80	17.00	28.10	34.50
27-Jan-93	5.60	8.40	10.00	12.40	16.50	17.90	18.60	24.70	42.60	43.10
22-Mar-93	4.90	7.30	8.90	10.00	14.50	18.40	19.60	19.80	20.10	21.50
15-Apr-93	1.80	2.70	3.50	4.90	7.20	13.40	19.20	21.20	21.20	21.20
20-Aug-93	1.20	1.80	2.20	3.00	5.00	6.90	7.10	9.60	17.60	20.60
9-Sep-93	1.30	1.90	2.50	3.50	6.10	7.20	8.10	10.80	13.00	15.20
10-Nov-93	4.10	4.80	4.90	5.50	7.00	7.10	7.10	13.20	13.30	18.90
29-Dec-93	3.50	5.00	5.70	6.30	6.40	7.30	10.20	17.00	19.10	25.60
18-Jan-94	3.30	4.60	5.30	7.90	13.60	19.20	20.40	24.00	25.50	25.90

Table 4 Maximum Precipitation for different time periods (Millipunku station)

	Duration in minutes									
Date	15	20	30	45	60	120	180	360	720	1440
8-Jun-90	6.00	6.90	6.00	5.60	7.20	5.75	4.70	2.48	1.70	1.54
26-Sep-90	8.40	8.40	7.00	6.40	9.40	8.15	6.57	3.92	1.96	1.00
31-Dec-90	32.80	32.70	25.40	18.67	15.40	8.00	5.47	2.82	1.53	0.95
25-Jan-91	26.00	24.60	17.00	12.13	9.80	6.85	4.77	2.82	1.44	1.17
12-Aug-91	24.80	23.10	15.80	10.80	11.00	9.15	6.50	3.27	1.63	1.23
13-Mar-91	7.60	8.10	6.00	5.07	7.20	6.00	4.77	3.17	1.82	0.93
2-Nov-91	8.40	9.00	7.60	7.47	8.70	7.45	6.30	3.57	1.95	1.02
26-Nov-91	7.20	6.30	4.80	3.87	5.30	3.30	2.33	1.62	1.25	0.84
4-Dec-91	11.60	12.90	11.20	10.27	11.00	7.00	4.90	2.88	1.85	1.36
6-Jan-92	11.60	13.20	10.00	8.27	6.80	4.75	3.57	1.87	1.11	0.97
15-Jan-92	6.00	6.90	6.00	5.87	6.60	3.55	2.57	1.42	1.07	0.85
14-Feb-92	13.20	14.70	13.20	11.33	10.00	6.80	4.70	2.35	1.60	0.81
22-Nov-92	10.80	10.80	9.20	8.67	11.40	7.80	5.67	3.02	2.39	2.00
7-Dec-92	12.80	12.60	10.00	10.13	10.20	7.50	5.93	4.03	2.18	1.23
10-Jan-93	16.40	18.30	16.40	15.73	22.20	14.15	9.77	4.88	2.44	1.22
19-Jan-93	18.80	21.30	17.00	15.20	15.10	8.40	5.60	2.83	2.34	1.44
27-Jan-93	22.40	25.20	20.00	16.53	16.50	8.95	6.20	4.12	3.55	1.80
22-Mar-93	19.60	21.90	17.80	13.33	14.50	9.20	6.53	3.30	1.68	0.90
15-Apr-93	7.20	8.10	7.00	6.53	7.20	6.70	6.40	3.53	1.77	0.88
20-Aug-93	4.80	5.40	4.40	4.00	5.00	3.45	2.37	1.60	1.47	0.86
9-Sep-93	5.20	5.70	5.00	4.67	6.10	3.60	2.70	1.80	1.08	0.63
10-Nov-93	16.40	14.40	9.80	7.33	7.00	3.55	2.37	2.20	1.11	0.79
29-Dec-93	14.00	15.00	11.40	8.40	6.40	3.65	3.40	2.83	1.59	1.07
18-Jan-94	13.20	13.80	10.60	10.53	13.60	9.60	6.80	4.00	2.13	1.08

Table 5 Maximum Intensities for different time periods (Millipunku station)

The Gumbel distribution is widely used for hydrological purposes, especially for extreme events. (Chow V. et al., 1994) and it was used to define its statistics values. The formulas that define the Gumbel distribution are:

$$x_T = \mu + \alpha \cdot \left(-\ln\left(\ln \frac{T}{T-1} \right) \right)$$ **Eq. 7**

$$\mu = Xs - 0.5772 \cdot \alpha$$ **Eq. 8**

$$\alpha = \frac{\sqrt{6} \cdot s}{\pi}$$ **Eq. 9**

Where:

x_T is the intensity (mm/hr) for a defined return period

μ is a statistic position parameter known as the mode

Xs is the average of the intensity record

α is a scale parameter

s is the standard deviation of the intensity records

T is the return period in years

Applying these formulas it is possible to obtain the Gumbel distribution parameters shown in Table 6.

	Duration in minutes									
	15	20	30	45	60	120	180	360	720	1440
Standard deviation S and Average intensity Xm (mm/hr)										
Xm	13.55	14.14	11.19	9.45	10.15	6.80	5.04	2.93	1.78	1.11
S	7.39	7.37	5.54	4.16	4.25	2.61	1.83	0.91	0.56	0.33
Scale parameter α and position parameter μ										
α	5.76	5.75	4.32	3.24	3.31	2.03	1.43	0.71	0.44	0.26
μ	10.22	10.82	8.70	7.58	8.24	5.63	4.21	2.52	1.52	0.96

Table 6 Gumbel distribution parameters

Based on this table the intensities and precipitation for different return periods were calculated. The results are shown in Table 7.

Intensity (mm/hr)

	Duration in minutes									
T (years)	15	20	30	45	60	120	180	360	720	1440
5	18.9	19.4	15.2	12.4	13.2	8.7	6.4	3.6	2.2	1.3
10	23.2	23.7	18.4	14.9	15.7	10.2	7.4	4.1	2.5	1.5
25	28.7	29.2	22.5	17.9	18.8	12.1	8.8	4.8	2.9	1.8
50	32.7	33.2	25.6	20.2	21.2	13.6	9.8	5.3	3.2	2.0
100	36.7	37.2	28.6	22.5	23.5	15.0	10.8	5.8	3.5	2.1

Precipitation (mm)

	Duration in minutes									
T (years)	15	20	30	45	60	120	180	360	720	1440
5	4.7	6.5	7.6	9.3	13.2	17.4	19.1	21.5	26.1	32.2
10	5.8	7.9	9.2	11.2	15.7	20.4	22.3	24.7	30.0	36.9
25	7.2	9.7	11.3	13.5	18.8	24.3	26.3	28.7	35.0	42.7
50	8.2	11.1	12.8	15.2	21.2	27.1	29.3	31.7	38.7	47.0
100	9.2	12.4	14.3	16.9	23.5	30.0	32.3	34.7	42.3	51.3

Table 7 Intensities and precipitation values for different return periods (Millipunku station)

The resulting graphs from Table 7 are show in Figure 13 and Figure 14. In both figures it can be noticed the non uniformity of the curves as it should be expected. This is due to the record period which becomes too short to get a reliable statistic analysis from the intensities record.

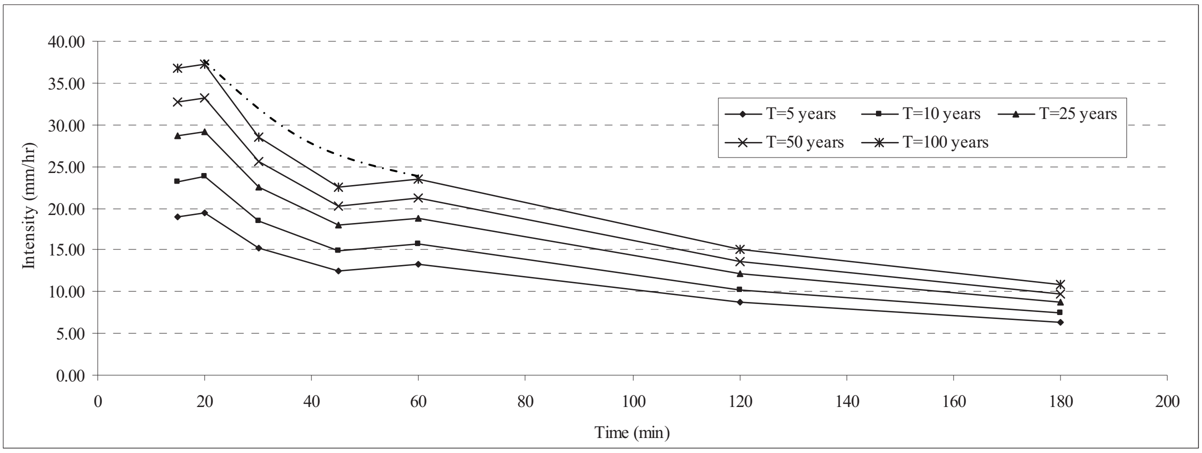

Figure 13 Intensity-Duration-Frequency curves for the Achumani catchment

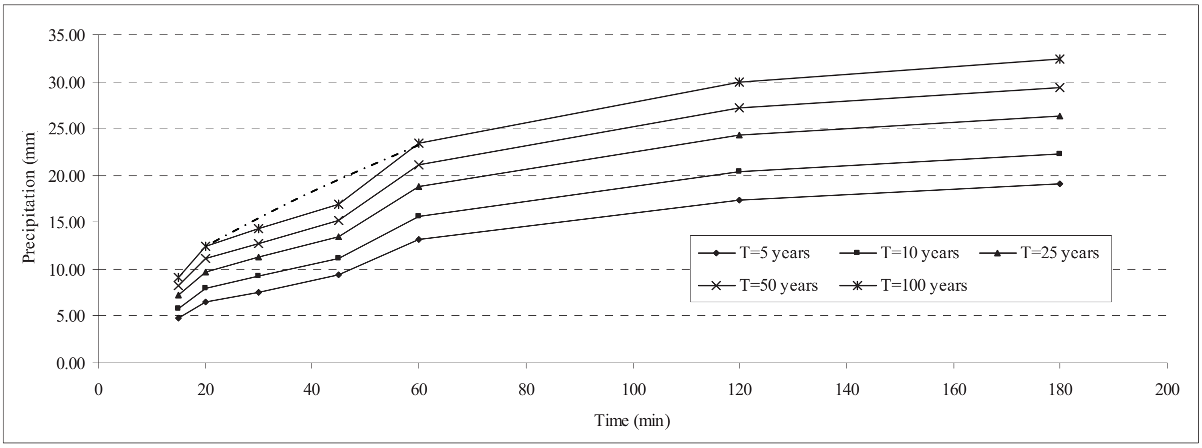

Figure 14 Precipitation-Duration-Frequency curves for the Achumani catchment

Using Figure 13 a six hour design hyetograph was determined using a return period of 100 years. This design hyetograph was determined using the alternate blocking criteria (Chow V. et al., 1994). The final result is presented in Table 8 and Figure 15

Duration	Intensity	Cumul Depth	Increm Depth	Time	Increm. Depth	Block Precip
min	mm/hr	mm	mm	hr	mm	mm
15	36.73	9.18	9.18	0 - 15	9.18	0.42
30	28.57	14.29	5.10	15 - 30	5.10	0.71
45	22.49	16.87	2.58	30 - 45	2.58	0.90
60	23.47	23.47	6.60	45 - 60	6.60	2.58
75	21.00	26.25	2.78	60 - 75	2.78	5.10
90	19.00	28.50	2.25	75 - 90	2.25	9.18
105	16.80	29.40	0.90	90 - 105	0.90	6.60
120	14.98	29.96	0.56	105 - 120	0.56	2.78
135	13.50	30.38	0.42	120 - 135	0.42	2.25
150	12.30	30.75	0.38	135 - 150	0.38	0.88
165	11.50	31.63	0.88	150 - 165	0.88	0.56
180	10.78	32.33	0.71	165 - 180	0.71	0.38

Table 8 Design hyetograph using the Millipunku 100 return period IDF curve

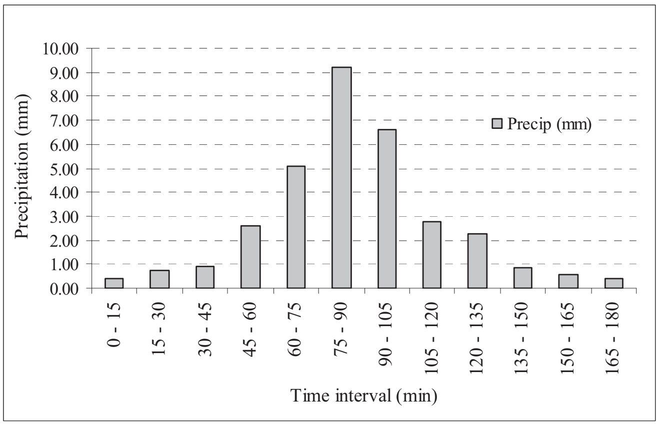

Figure 15 Block precipitation distribution based on Millipunku IDF curve

As it was mentioned in the first part of Section 4.2 the performance of the design hyetogram presented in Figure 15 will be assessed with the hyetograph obtained using the distribution coefficients defined by Mendoza (2000) for the San Calixto station, and applying them to the maximum precipitation values presented in Table 7.

	P24	Distribution coefficients Pd/P24 max									
T(years	(mm)	Duration (min)									
		15	20	30	45	60	120	180	360	720	1440
5	37.4	0.181	0.225	0.299	0.383	0.447	0.6	0.682	0.803	0.902	1
10	43	0.184	0.229	0.306	0.394	0.461	0.621	0.706	0.828	0.921	1
25	50	0.188	0.235	0.313	0.404	0.472	0.635	0.722	0.845	0.939	1
50	55.2	0.189	0.237	0.317	0.41	0.48	0.65	0.739	0.861	0.949	1
100	60.4	0.191	0.239	0.32	0.414	0.485	0.657	0.746	0.87	0.957	1

Table 9 Distribution coefficients for the San Calixto station (Mendoza, 2000)

	Duration in minutes									
T (years)	15	20	30	45	60	120	180	360	720	1440
5	5.8	7.3	9.6	12.3	14.4	19.3	22.0	25.9	29.1	32.2
10	6.8	8.4	11.3	14.5	17.0	22.9	26.0	30.5	33.9	36.9
25	8.0	10.0	13.4	17.2	20.2	27.1	30.8	36.1	40.1	42.7
50	8.9	11.1	14.9	19.3	22.6	30.6	34.8	40.5	44.6	47.0
100	9.8	12.3	16.4	21.3	24.9	33.7	38.3	44.7	49.1	51.3

Table 10 Precipitation values for different return periods using San Calixto distribution coeffcients

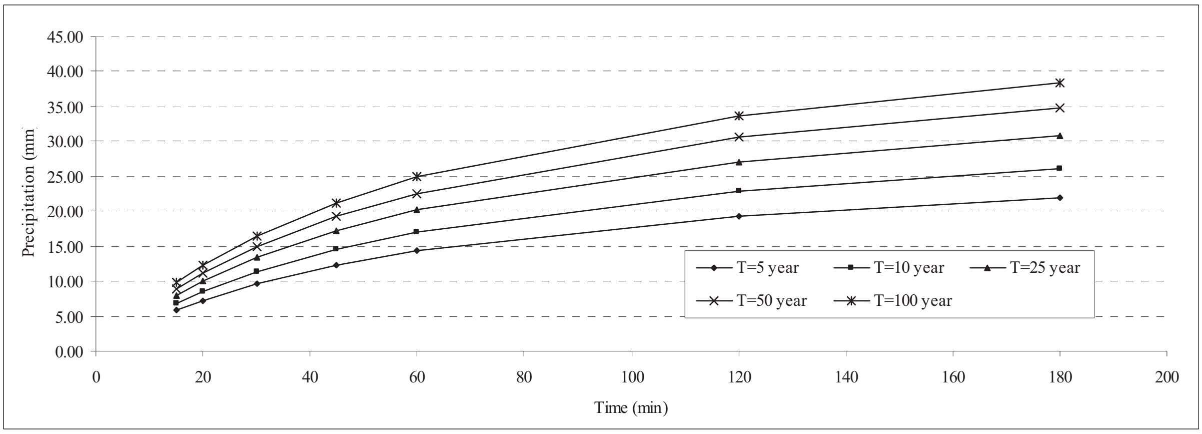

Figure 16 Precipitation-Duration-Frequency curves based on the distribution coeffcients from San Calixto station

Using the same methodology as for the design hyetograph using the Millipunku PDF, the design hyetograph based on San Calixto distribution coefficients is presented in Table 11 and Figure 18.

Duration	Intensity	Cumul Depth	Increm Depth	Time	Increm. Depth	Block Precip
min	mm/hr	mm	mm	hr	mm	mm
15	39.22	9.80	9.80	0 - 15	9.80	0.80
30	32.85	16.43	6.62	15 - 30	6.62	1.58
45	28.34	21.25	4.83	30 - 45	4.83	1.98
60	24.90	24.90	3.64	45 - 60	3.64	3.60
75	22.80	28.50	3.60	60 - 75	3.60	4.83
90	20.50	30.75	2.25	75 - 90	2.25	9.80
105	18.70	32.73	1.98	90 - 105	1.98	6.62
120	16.86	33.73	1.00	105 - 120	1.00	3.64
135	15.20	34.20	0.47	120 - 135	0.47	2.25
150	14.00	35.00	0.80	135 - 150	0.80	1.72
165	13.30	36.58	1.58	150 - 165	1.58	1.00
180	12.76	38.29	1.72	165 - 180	1.72	0.47

Table 11 Design hyetograph using the San Calixto 100 return period distribution coefficients

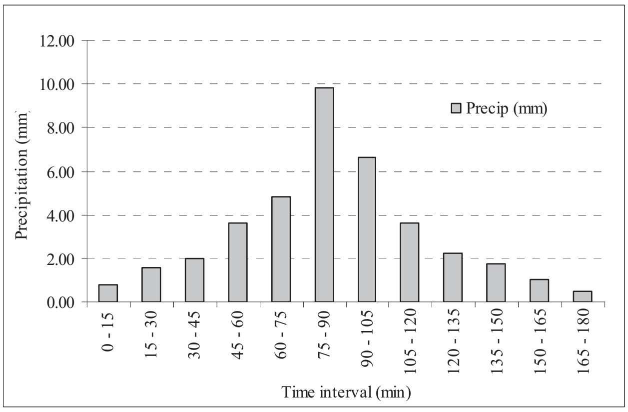

Figure 17 Block precipitation distribution based on San Calixto distribution coefficients

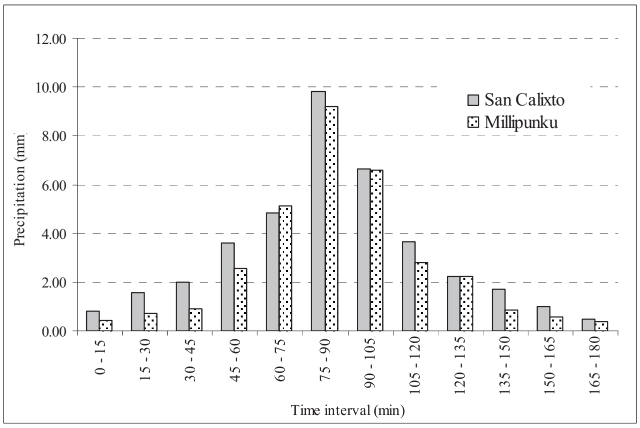

Figure 18 Design hyetographs based on Millipunku station and San Calixto station

Figure 15 and Figure 17 show the final design hyetographs for a return period of 100 years. These hyetographs will be used to calculate the design discharge values using the unit hydrograph derived from the GIUH modelling.

Figure 18 shows the difference between the two design hyetographs. Based on San Calixto station the maximum precipitation estimated is about 7% higher than Millipunku station. This analysis is important because despite the short record period for the Millipunky station there is an acceptable correlation between them. However, the variation at the beginning of the graph as at the end is more considerable.

This same methodology was followed to obtain the design hyetographs for 50 years of return period shown in Table 12.

Time (min)	15	30	45	60	75	90	105	120	135	150	165	180
Block Precip Millipunku station	0.30	0.83	1.02	2.39	4.60	8.18	5.99	2.59	2.20	0.87	0.33	0.05
Block Precip San Calixto ditr. Coeff.	0.93	1.21	1.80	2.93	4.37	8.89	6.02	3.29	2.55	1.53	1.00	0.25

Table 12 Design hyetograph for 50 years return period

4.3. Land cover-use map

Land cover and land use survey were made in order to generate the land cover-use map. The effective (excess) rainfall is computed according to the Soil Conservation Service (SCS) runoff method (Patil et al., 2008) In order to find the adequate values for the initial abstraction (P_0), the land use map, land cover map and soil map are needed. Using GIS techniques, a representative P_0 for the Achumani catchment was determined.

According to the field survey, eight categories were defined for the land cover-use classification. They were selected based on Ferrer (2006) who made a relation among approximately 150 land use types with its equivalence to the land use necessary for the SCS methodology. Figure 19 shows four different scenarios from the eight that were selected for this map classification

- Areas with poor vegetation
- River bed
- Constructed areas with vegetation between 50-75%
- Badlands and/or erosive areas
- Natural Pastures
- Poor Forest
- Short meadows
- Urban areas

a) Areas with natural scarse vegetation

b) Badlands and/or erosive areas

c) Urban Areas

d) River bed

Figure 19 Different land cover and land use scenarios in the Achumani catchment

The criteria used to define the land cover-use map were based on information obtained from the following sources:.

- Field survey and GPS ground control points for spatial location of the units.
- High resolution imagery (Quickbird and aerial orthophotos)

Figure 20 shows the final map product of this classification. It can be seen that most part of the catchment presents areas with poor vegetation. The erosive areas also play an important role in this classification.

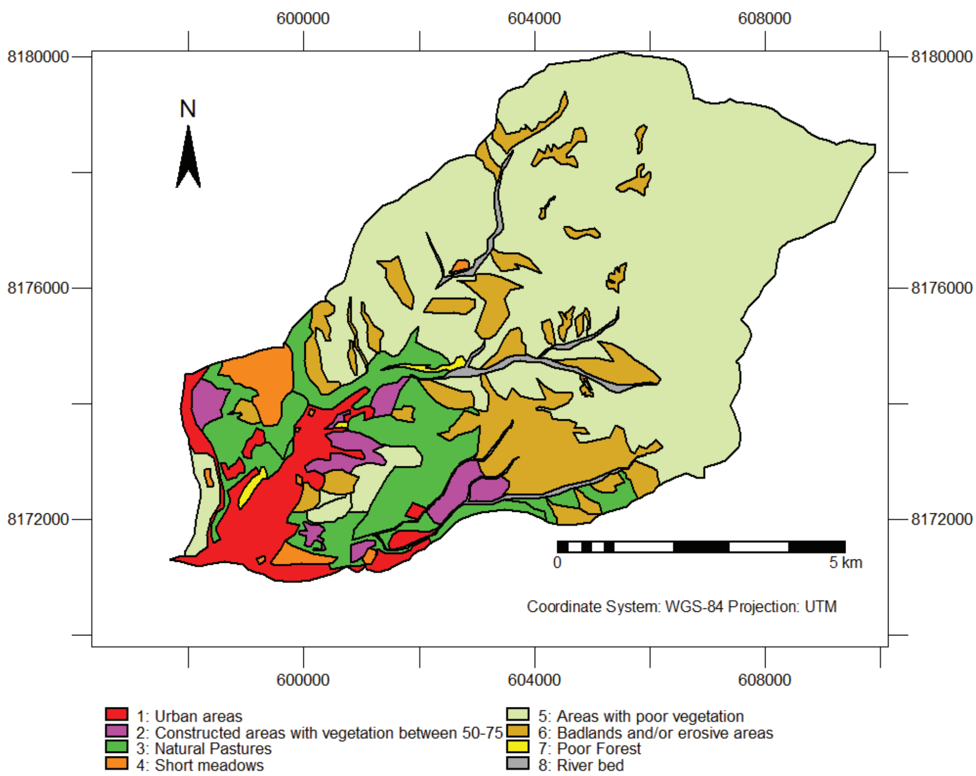

Figure 20 Land cover-use map for the Achumani catchment

4.4. Infiltration process

In the practice, the estimation of the water losses or abstractions can be presented in two cases. When precipitation and discharge information is available or with precipitation only. In the first case, non-linear programming methods can be used or a simple method such as the phi index. In the second case, methods based on infiltration equations can be used (Green Ampt, Horton, Philip, etc) or the method proposed by the National Conservation Service (SCS), which is recommended for ungauged catchments.

4.4.1. Effective Rainfall according to the SCS method

The Curve Number Method was originally developed by the Soil Conservation Service for conditions prevailing in the United States. Since then, it has been adapted to conditions in other parts of the world. Although some regional research centres have developed additional criteria, the basic concept is still widely used all over the world. (Chow V. et al., 1994)

The effective rainfall is expressed by:

$$P_n = \frac{(P - P_0)^2}{P + 4P_0} \quad \textbf{Eq. 10}$$

Where:

P = Total precipitation registered

P_n = Effective rainfall

P_0 = Initial abstraction

The initial abstraction P_0 represents interception, depression storage, and infiltration before the start of runoff. This parameter depends on the soil type (A, B, C, D) and the antecedent moisture condition (AMC(I), AMC(II), AMC(III)). The initial abstraction values used for this study and a further explanation of the effective rainfall methodology proposed by the SCS (Soil Conservation Service) can be found in Appendix 3

The initial abstraction values were defined according to the land use classification and the values suggested by Ferrer (2006). The selection of the initial abstraction value depends on the antecedent moisture condition (AMC) and the hydrological soil group.

According to the explanation given in Section 4.1 where it was discussed the type of soil and the selected rainfall event for the model, the selected hydrological soil group is B and AMC(III).

Using the land cover-use map and the conversion equations cited the following table was defined.

Land-Soil Unit	**Area A_0 (km^2)**	**Ao/At**	**Initial Abstraction P_0(III)**	**Ponded P_0 P_0*Ao/At**
Areas with poor vegetation	37.33	0.59	6	3.6
River bed	1.11	0.02	2	0.0
Constructed areas with vegetation between 50-75%	2.05	0.03	6	0.2
Badlands and/or erosive areas	8.70	0.14	3	0.5
Natural Pastures	7.67	0.12	6	0.7
Poor Forest	0.25	0.00	7	0.0
Short meadows	1.40	0.02	10	0.2
Urban areas	4.30	0.07	0	0.0
Total Area	**At = 62.81**		**Σ P_0**	**5.3**

Table 13 Initial abstraction value for the Achumani catchment

Hours	**P (mm)**	**ΣP (mm)**	**ΣPn (mm)**	**Pn**
1	0.0	0.00	0.00	**0.00**
2	6.0	6.00	0.04	**0.04**
3	0.0	6.00	0.04	**0.00**
4	0.0	6.00	0.04	**0.00**
5	0.0	6.00	0.04	**0.00**
6	2.1	8.10	0.34	**0.30**
7	0.1	8.20	0.36	**0.02**
8	0.2	8.40	0.41	**0.04**
9	0.0	8.40	0.41	**0.00**
10	0.0	8.40	0.41	**0.00**
11	1.5	9.90	0.80	**0.40**
12	0.2	10.10	0.86	**0.06**
13	0.2	10.30	0.93	**0.06**
14	0.1	10.40	0.96	**0.03**
15	0.3	10.70	1.06	**0.10**
16	0.2	10.90	1.13	**0.07**
17	0.1	11.00	1.16	**0.03**

Table 14 Effective rainfall according to the SCS methodology

Based on the initial abstraction calculated in Table 13 effective rainfall calculation can be made. For this purpose the precipitation data shown in Figure 12 and the initial abstraction were used. Table 14 will be used as the precipitation input data for the GIUH modelling process.

4.4.2. The Phi index method

The phi index is defined as a constant abstraction rate in mm/hr, which will produce an effective hyetograph with a total precipitation equal to the total surface runoff over the catchment, r_d (Nania, 2002)

$$r_d = \sum_{m=1}^{M} (R_m - \phi \cdot \Delta t) \quad \textbf{Eq. 11}$$

Where:

R_m is the observed precipitation (mm) in the time interval m (refered to the time interval where there is response to rainfall) and Δt is the time interval (hrs)

Using the precipitation and the discharge measurements data presented in Figure 12, Table 15 was developed.

The first step to define the table is to estimate the baseflow value. In this case and looking at the hydrograph in Figure 12 a baseflow of 0.17 m^3/s was chosen because after this discharge value there is a direct response to rainfall. So this baseflow value was subtracted from the hydrogram..

The total runoff volume V_d and the effective rainfall volume r_d need to be calculated. Vd is obtained calculating the integer below the direct runoff hydrograph.

$$V_d = \sum_{m=1}^{28} Q_d \cdot \Delta t = 19.4 \frac{m^3}{s} \cdot 1hr \cdot \frac{3600s}{1hr} = 69976.8m^3$$

To calculate r_d the total runoff volume is divided by the catchment area. (Refer to Section 4.1)

$$r_d = \frac{V_d}{A} = \frac{69976.8m^3}{68.2 \cdot 10^6 m^2} = 1.03 \cdot mm$$

All the rainfall before the surface runoff generation will be considered initial abstraction, this means all rainfall before 4-15 (See Table 15). The abstraction ratio ϕ and the number of intervals from the effective runoff hyetograph are found by trial and error, selecting the highest rainfall value in the effective runoff period and calculating r_d to find ϕ..

The first iteration: M=1. The highest precipitation volume is chosen (1.5 mm) using:

$$r_d = \sum_{m=1}^{M} (R_m - \phi \cdot \Delta t) = 1.03mm = (1.5mm - \phi \cdot 1hr) \Rightarrow \phi = 0.47mm/hr$$

This final value represents an abstraction of 0.47 mm for 1 hour interval. This value is subtracted from the total precipitation volume, resulting in this way the final effective rainfall hyetograph.

Time	Observed data		Effective rainfall	Direct runoff hydrogram
	Precipitation	Discharge		
Day-Hour	mm	m^3/s	mm	m^3/s
4-9	0.0	0.15		
4-10	6.0	0.17	5.53	
4-11	0.0	0.17		
4-12	0.0	0.17		
4-13	0.0	0.17		
4-14	2.1	0.17	1.63	
4-15	0.1	1.64		1.47
4-16	0.2	0.9		0.73
4-17	0.0	0.532		0.362
4-18	0.0	0.4		0.23
4-19	1.5	1.8	1.03	1.63
4-20	0.2	2.08		1.91
4-21	0.2	2.41		2.24
4-22	0.1	2.33		2.16
4-23	0.3	1		0.83
5-0	0.2	1.18		1.01
5-1	0.1	1.1		0.93
5-2		1.23		1.06
5-3		1.07		0.9
5-4		0.48		0.31
5-5		0.55		0.38
5-6		0.77		0.6
5-7		0.643		0.473
5-8		0.643		0.473
5-9		0.56		0.39
5-10		0.48		0.31
5-11		0.4		0.23
5-12		0.3		0.13
5-13		0.3		0.13
5-14		0.29		0.12
5-15		0.29		0.12
5-16		0.28		0.11
5-17		0.27		0.1
5-18		0.27		0.1
			Σ	**19.4**

Table 15 Effective rainfall according to the Phi index method

4.4.3. The Kostiakov model

Kostiakov (1932) proposed a simple empirical infiltration equation based on curve fitting from field data. It relates infiltration to time as a power function:

$f_p = K_k \cdot t^{-\alpha}$ **Eq. 12**

Where:

fp = infiltration capacity [Lt^{-1}],

t = time after infiltration starts [t], and

K_k [L] and α [unitless] are constants that depend on the soil and initial conditions.

The parameters, K_k and α must be evaluated from measured infiltration data, since they have no physical interpretation. The equation describes the measured infiltration curve and given the same soil and same initial water condition, allows prediction of an infiltration curve using the same constants developed for those conditions.

The Kostiakov equation is widely used because of its simplicity, ease of determining the two constants from measured infiltration data and reasonable fit to infiltration data for many soils over short time periods. (Turner, 2006)

The major flaws of this equation are that it predicts that the infiltration capacity is infinite at t equals zero and approaches zero for long times, while actual infiltration rates approach a steady value. Based on this approach Mezencev (1948) proposed a modification to Kostiakov's equation by adding a constant f_c to the equation that represents the final infiltration rate reached when the soil becomes saturated after prolonged infiltration.

$f_p = K_k \cdot t^{-\alpha} + f_c$ **Eq. 13**

To estimate the values for K_k and α a logarithmic form of the equation is used.

The detail for the least square fit equations can be found in Appendix 4

PCA (2007) made infiltration measurements in the Achumani catchment using double ring infiltrometers. A total of eight measurements were made over the La Paz catchment. From these, only one of the tests belongs to the Achumani catchment. Table 16 shows this data and the least square fit made.

Accumulated time (min)	Partial time	Real accumulated infiltration F_p (mm)	Real instantaneous infiltration f_p (mm/hr)	Calculated accumulated infiltration F_p calc (mm)	Calculated instantaneous Infiltration F_p (mm/h)	y=log F_p	x^2=(log t)^2	x=log t	xy=log F_p*log t
0	0	0.00		0.00	0.00				
0.85	0.85	20.00	1411.76	21.35	832.81	1.30	0.00	-0.07	-0.09
2.90	2.05	40.00	585.37	42.46	497.80	1.60	0.21	0.46	0.74
5.47	2.57	60.00	467.53	60.90	381.60	1.78	0.54	0.74	1.31
8.85	3.38	80.00	354.68	80.23	311.80	1.90	0.90	0.95	1.80
13.83	4.98	100.00	240.80	103.68	258.54	2.00	1.30	1.14	2.28
17.13	3.30	120.00	363.64	117.26	236.36	2.08	1.52	1.23	2.57
21.68	4.55	140.00	263.74	134.30	214.13	2.15	1.79	1.34	2.87
27.77	6.08	160.00	197.26	154.87	193.04	2.20	2.08	1.44	3.18
34.23	6.47	180.00	185.57	174.76	176.81	2.26	2.35	1.53	3.46
41.95	7.72	200.00	155.51	196.53	162.37	2.30	2.63	1.62	3.73
50.62	8.67	220.00	138.46	219.05	150.07	2.34	2.90	1.70	3.99
60.92	10.30	240.00	116.50	243.81	138.86	2.38	3.19	1.78	4.25
71.87	10.95	260.00	109.59	268.27	129.56	2.41	3.45	1.86	4.48
83.47	11.60	280.00	103.45	292.53	121.68	2.45	3.69	1.92	4.70
94.50	11.03	300.00	108.76	314.32	115.51	2.48	3.90	1.98	4.89
					Σ	31.63	30.47	19.63	44.17

Table 16 Least square fit for the infiltration measurements

Applying the equations for K_k and α the following equation was found.

Instantaneous infiltration rate (mm/hr) $f_p = 777.94 \cdot t^{-0.42}$ (t in minutes)

Accumulated infiltration (mm) $F_p = 22.33 \cdot t^{0.58}$ (t in minutes)

Average infiltration rate (mm/hr) $f_p = 22.33 \cdot t^{-0.42}$ (t in minutes)

Figure 21 shows the infiltration curves resulting from the Kostiakov infiltration model

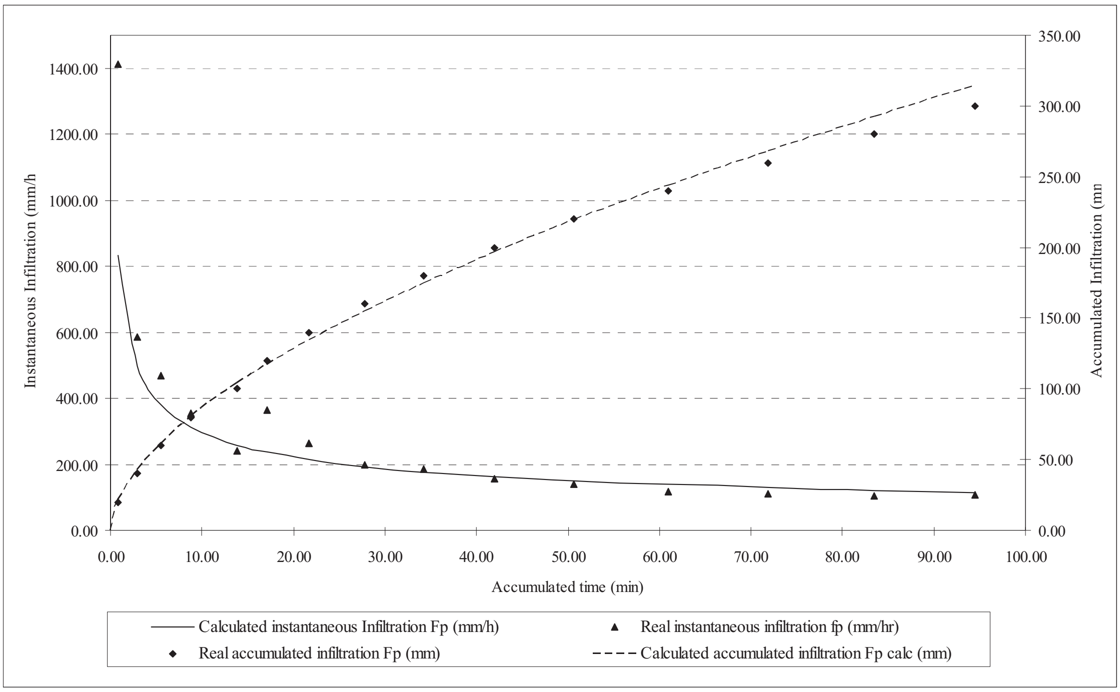

Figure 21 Double ring infiltrometer plot based on Kostiakov model (PCA Consulting Engineers and NIPPON KOEI CO. LTD., 2007)

From the results obtained we can see that the infiltration rates calculated are relatively high. If we compare these results to the total precipitation of the event to be modelled, it means that all the precipitation should be infiltrated. Unfortunately, this infiltration test is the only data available but, due to these results, the type of soil over the area and the dry period in which it was made, we can’t assume it is applicable to the situation of this storm.

4.5. DEM processing

4.5.1. Introduction

A Digital Elevation Model (DEM) is one of the most useful sources of information for spatial modelling and monitoring. The great applicability of this information goes from Environment and Earth Science (e.g. catchment dynamics and the prediction of soil properties), Engineering (e.g. road construction and wind turbine location optimisation); Military (e.g. land surface visualisation); etc. The extraction of land surface parameters – whether they are based on ‘bare earth’ models such as DTM derived from contour lines and spot heights, or ‘surface cover’ models derived from remote sensing sources that include tree top canopies and buildings for example – is becoming more common and more attractive due to the increasing availability of high quality and high resolution DEM data. (Reuter H.I et al., 2007)

As it was mentioned in one of the specific objectives of this study, the use of different DEM sources will be assessed in order to define the geomorphological characteristic needed for the GIUH modelling.

Three different DEM sources were selected:

- SRTM images
- Topographic maps

- Aerial photogrammetric restitution

4.5.2. SRTM images processing

Concept of hydrological modelling is broadly applied nowadays to represent a digital simulation of drainage systems based primarily on terrain analysis and performing automation extraction of the drainage networks (e.g. stream orders, catchment delineation, morphometric parameters)

One of the most important publicly available new spatial datasets in recent years is the Digital Elevation Model derived from the February 2000 Shuttle Radar Topography Mission (SRTM). The use of this information has been widely accepted due to its great range of applicability, especially for hydrological purposes (DEM extraction and geomorphological parameter extraction).

The image used for this study was derived from the USGS/NASA SRTM data[1]. The International Center for Tropical Agriculture (CIAT) has processed this data to provide seamless continuous topography surfaces. Areas with regions of no data in the original SRTM data have been filled using interpolation methods described by Reuter (2007). For georeferencing purposes and validation, a Landsat (June, 2002) image obtained from the Military Geographic Institute in Bolivia, was used.

In 2006, a complementary ground control point survey was made as part of the study made by PCA (PCA Consulting Engineers and NIPPON KOEI CO. LTD., 2007). During this study, 62 GPS points were measured and linked to the WGS-84 Bolivian National Geodesic Net. This information was used to assess the performance of the SRTM DEM to the La Paz catchment. The 62 height values were plotted against their corresponding SRTM points (Figure 22).

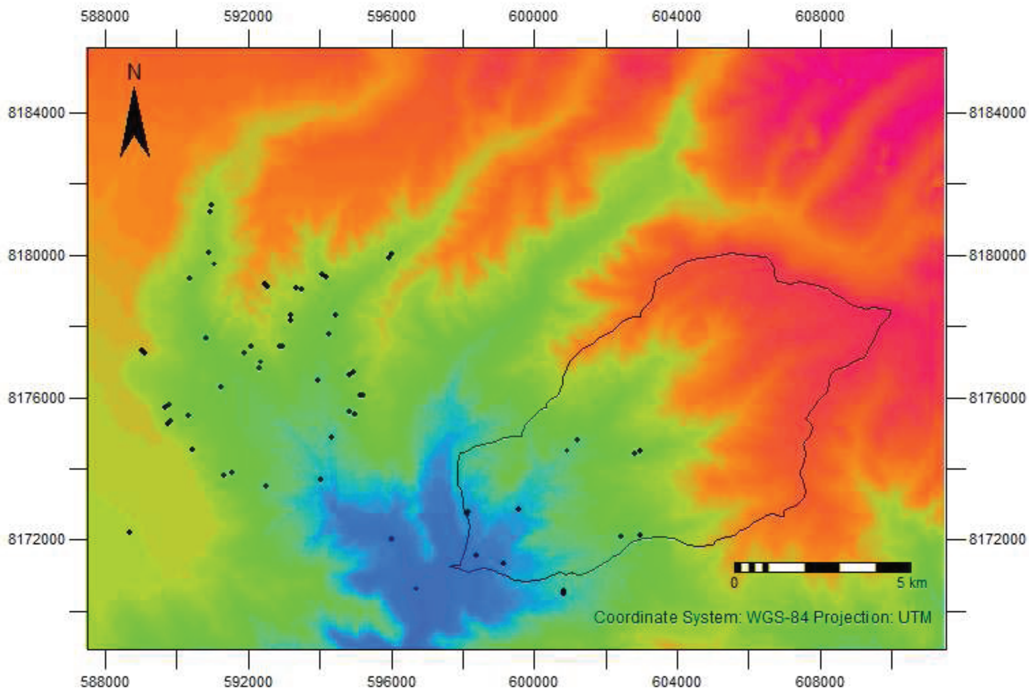

Figure 22 Ground Control Points distribution over La Paz catchment

[1] http://srtm.csi.cgiar.org/

These 62 points are located over the urban area of La Paz catchment and over the lower part of its five sub catchments. The resulting graph is shown in Figure 23.

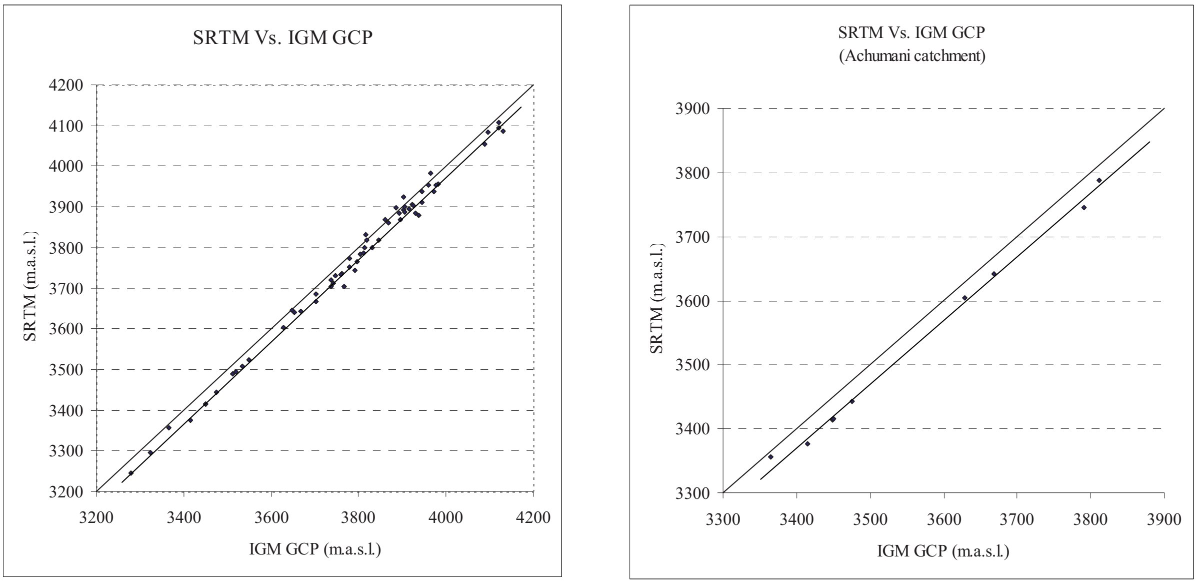

Figure 23 SRTM points compared with IGM Ground Control Points

As it can be seen, there is a high correlation between the SRTM points and the GCP points. Both point groups are shifted. There is an average distance of 30 m between these two surfaces that might be considered as a difference between the origins of the vertical datums. The points where the SRTM height values are higher or nearly close to the GCP is because they are located in urban areas with high buildings or in short areas with abrupt changes in topography

A similar situation occurs with the points located inside the Achumani catchment. From the nine points plotted there is one located in the lower part of the catchment (urban area) which SRTM height value is closer to the GCP height value. The other points have the same behaviour as explained in the previous paragraph. From this analysis we can conclude that there is an acceptable correlation between the SRTM height values and the GCP distributed over the catchment (the 30 meters of difference is just a parameter that establishes a vertical shift between both surfaces), thus the use of the SRTM for the DEM processing stage can be performed.

4.5.3. TOPOGRAPHIC maps processing

The 1:50.000 topographic maps collected during the fieldwork period were digitized and converted into a GIS platform. Using ILWIS the contour levels were interpolated in order to generate a 20 meters pixel size DEM. The criteria to use this pixel size is to have a medium resolution DEM, such as the one obtained from other satellite sources (e.g. Aster) Figure 24 shows the digitized contour levels previous to the interpolation process.

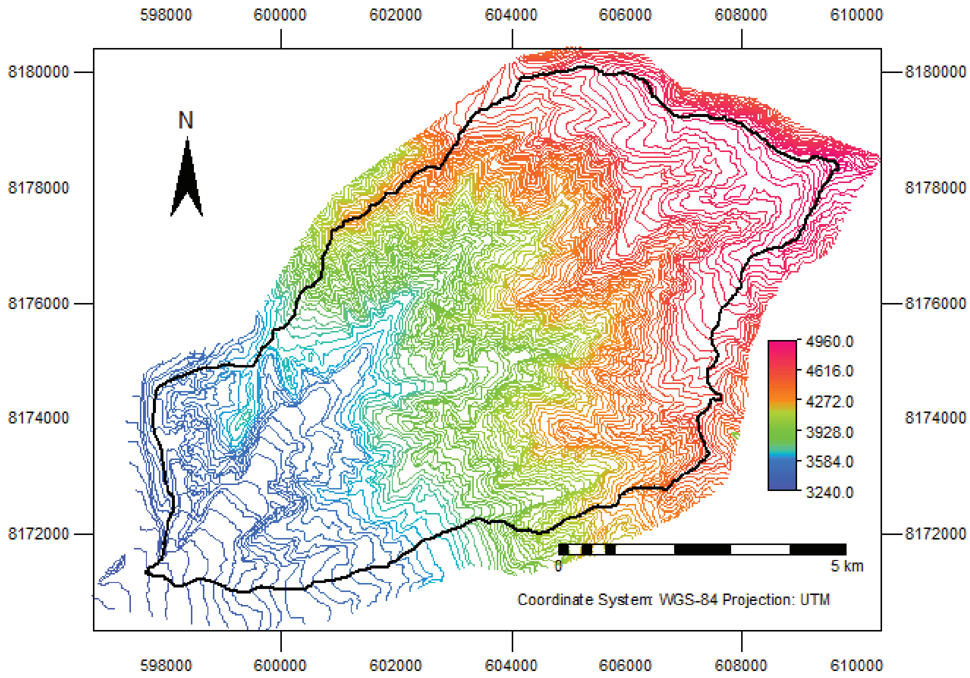

Figure 24 Digitized contour levels from IGM Topographic maps

4.5.4. Aerial orthophotos DEM processing

On 2006, the municipal government of La Paz city requested a new photogrammetric flight in order to update the city's cadastre. Based on that objective, the aereotriangulation and restitution process was developed using the photogrammetric stations based on Leica Photogrammetric Suit software. The Military Geographic institute was in charge of this project, which was finished on January 2008. The restitution covered: district, parcel, rivers, streets, avenues, green areas, areas of expansion and contour levels every meter. This contour level information will be used in this thesis to generate a high resolution DEM. Since this, information has not been disclosed yet in other public institutions, and these is the reason why it has not been yet used for other purposes such as hydrological processes.

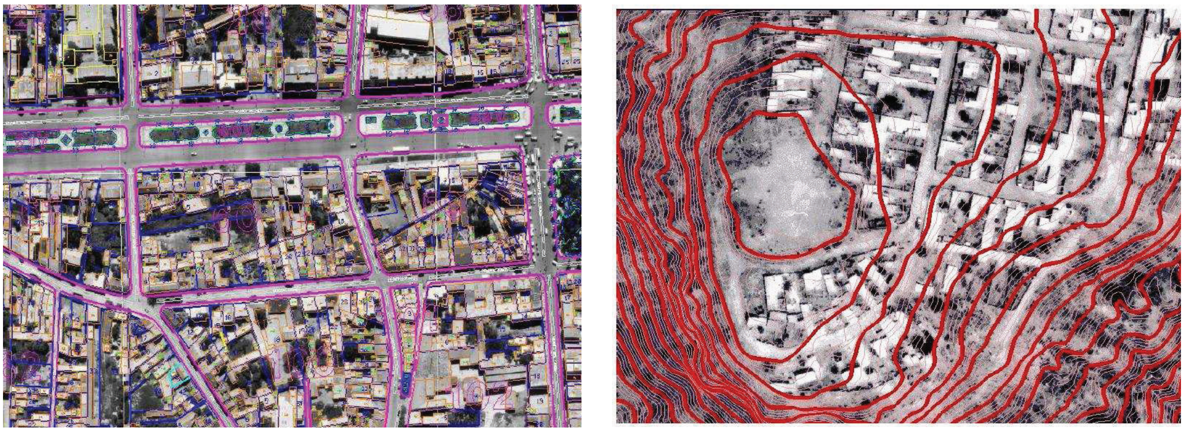

Figure 25 Aerial orthophotos restitution made for La Paz city

The contour interpolation process made for the aerial orthophotos restitution resulted in a high resolution DEM with 5 m pixel size.

4.6. DEM hydro-processing and statistical parameters extraction

4.6.1. Introduction

To work effectively with raster based elevation information a new routine has been developed using ILWIS, a GIS and RS package developed at ITC called the DEM hydro-processing module. This module supports further DEM processing to obtain a full raster and vector based (including topology) schematization of the (sub) catchments and drainage network, coupled with additional hydrological relevant parameters such as the Horton’s statistics. (Maathuis B.H.P. and Wang L., 2006)

The basic structure of the DEM hydro-processing module has been shown in Figure 6.

The next step towards the geomorphological parameter extraction is the Horton’s statistics parameter. The Horton Statistics operation calculates for each (Strahler) stream order number and for each merged catchment:

- The number of streams, N
- The average stream length L, and
- The average area of catchments A, and expected values for these by means of a least squares fit. N_LSq, L_LSq, A_LSq

The output is stored in a table which can be used to construct the so-called Horton plots. Horton plots enable the user to inspect the regularity of the extracted stream network based on the (Strahler) stream order numbers, and may serve as a quality control indicator for the entire stream network extraction process. It is expected that:

- The number of streams show a relative decrease for subsequent Strahler order numbers,
- The length of streams and the catchment areas show a relative increase for subsequent Strahler order numbers.

The results for the DEM hydro-processing stage and the Horton’s statistics are presented in the following sections.

4.6.2. SRTM DEM Hydro-processing

One of the most important variables to take into account for the drainage network extraction is the Stream threshold value. This variable represents the minimum number of pixels that should drain into the examined pixel in order to add this pixel to the output drainage network. The lower this value is the more segmented the drainage network. As it was mentioned in Section 3.1.2 around 100 GPS points located at the outlet of the main streams were collected for the drainage definition (Figure 5). The stream threshold value was defined looking the best fit between the drainage system and the GPS control points. For the SRTM DEM a threshold value of 12 pixels (97.200 m^2) was found to derive a more realistic drainage network. The final result from the DEM-hydro-processing (Figure 26) shows a 4^{th} order catchment according to the Strahler stream order. Table 17 is used to visualize the regularity of the stream network extracted according to the Horton’s ratios (refer to Section 3.2.1). The number of streams of successive order, the average stream length of successive order and the average catchment area of successive order is found to be relatively constant from one order to another (Maathuis B.H.P. and Wang L., 2006). Figure 27 shows the Horton’s statistics plot where it can be observed a good linearity between the Horton’s ratios values and the least square fit line plotted. This information and the final Horton ratios are presented in Table 17.

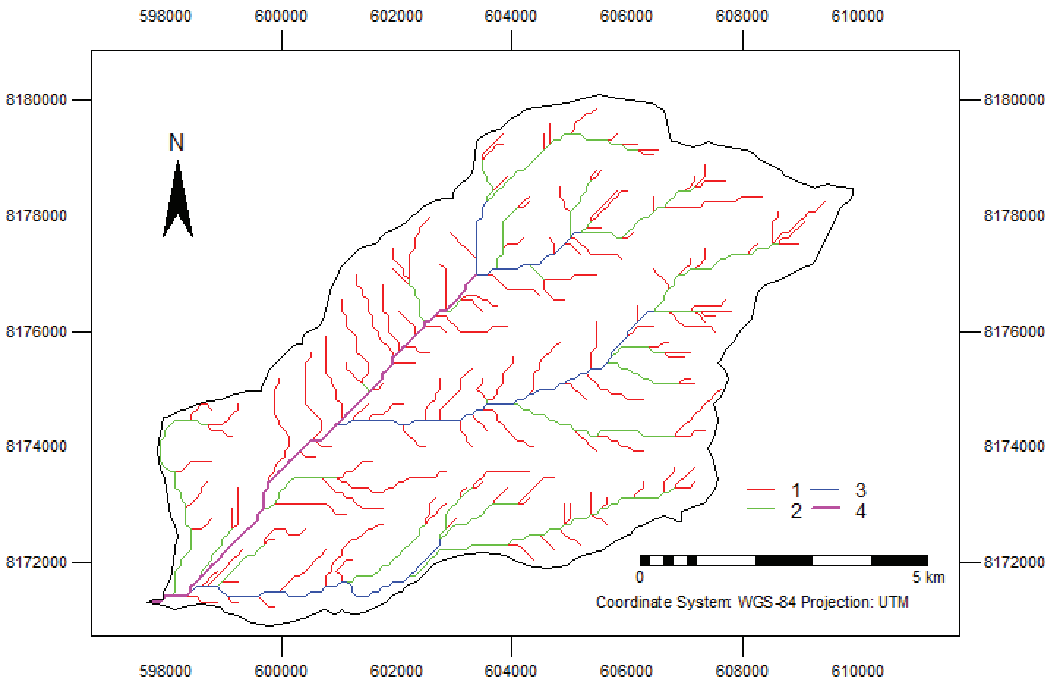

Figure 26 4th Strahler's stream order for the Achumani catchment (SRTM DEM)

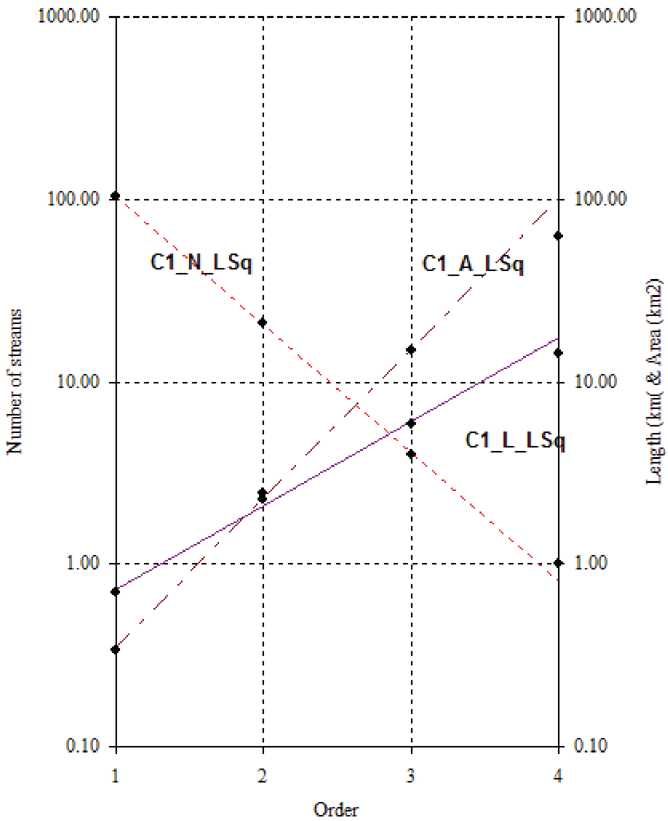

Figure 27 Horton's statistics plot for the SRTM DEM

Order	C1_N	C1_L	C1_A	C1_N_LSq	C1_L_LSq	C1_A_LSq
	(number)	(km)	(km2)	(number)	(km)	(km2)
1	103.00	0.70	0.34	104.16	0.73	0.35
2	21.00	2.26	2.46	20.53	2.10	2.31
3	4.00	5.84	14.80	4.05	6.06	15.26
4	1.00	14.38	62.73	0.80	17.51	100.70

Horton's Ratios		
Rb	Rl	Ra
5.07	2.89	6.6

Table 17 Horton statistics for SRTM DEM

4.6.3. TOPOGRAPHIC maps DEM Hydro-processing

Once the contour levels from the topographic maps were digitized, the DEM hydro-processing was made. In this case, the threshold stream value used was 250 pixels (100.000 m^2). Figure 28 shows the final drainage network ordering map. Following the same process described in Section 4.5.1 the resulting graphs for the Horton's statistics are shown in Figure 29 and Table 18.

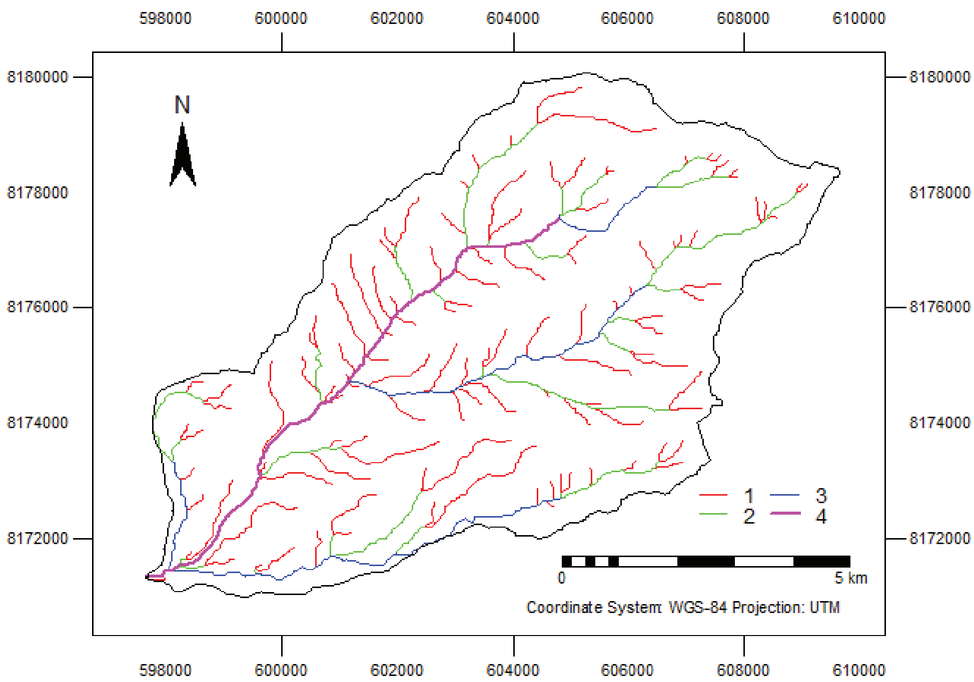

Figure 28 4th Strahler's stream order for the Achumani catchment (Topographic map DEM)

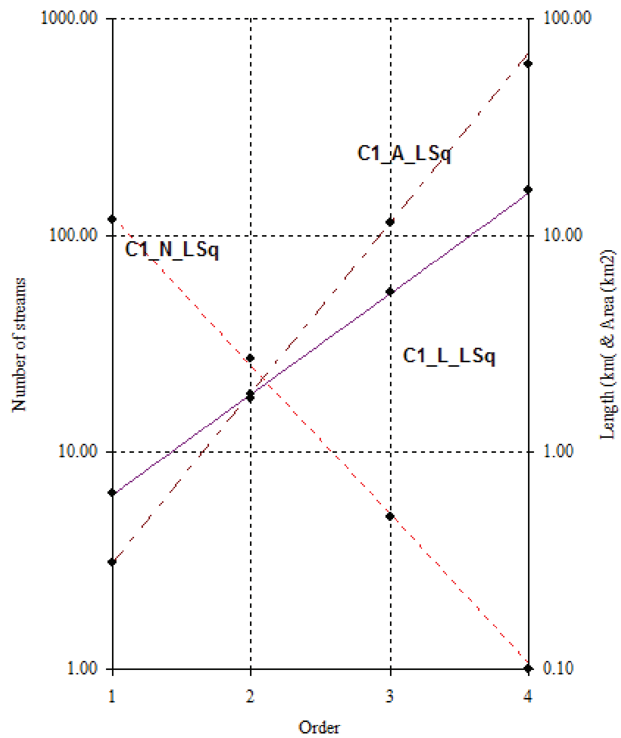

Figure 29 Horton statistics for Topographic map DEM

Order	C1_N (number)	C1_L (km)	C1_A (km2)	C1_N_LSq (number)	C1_L_LSq (km)	C1_A_LSq (km2)
1	118.00	0.65	0.31	122.24	0.64	0.31
2	27.00	1.76	1.85	25.16	1.85	1.88
3	5.00	5.49	11.50	5.18	5.36	11.42
4	1.00	16.16	61.78	1.07	15.59	69.57

Horton's Ratios		
Rb	**Rl**	**Ra**
4.95	2.94	5.88

Table 18 Horton statistics for Topographic maps DEM

4.6.4. Aerial orthophoto restitution DEM Hydro-processing

The DEM hydro-processing made to the aerial orthophoto restitution used a threshold stream value of 4000 (100.000 m^2). Due to the five meter pixel size and depending on the catchment area, the time consuming for this process can take up to three hours on a 1.83 GHz personal computer. Figure 31 and Table 19 show the final Horton statistics ratios.

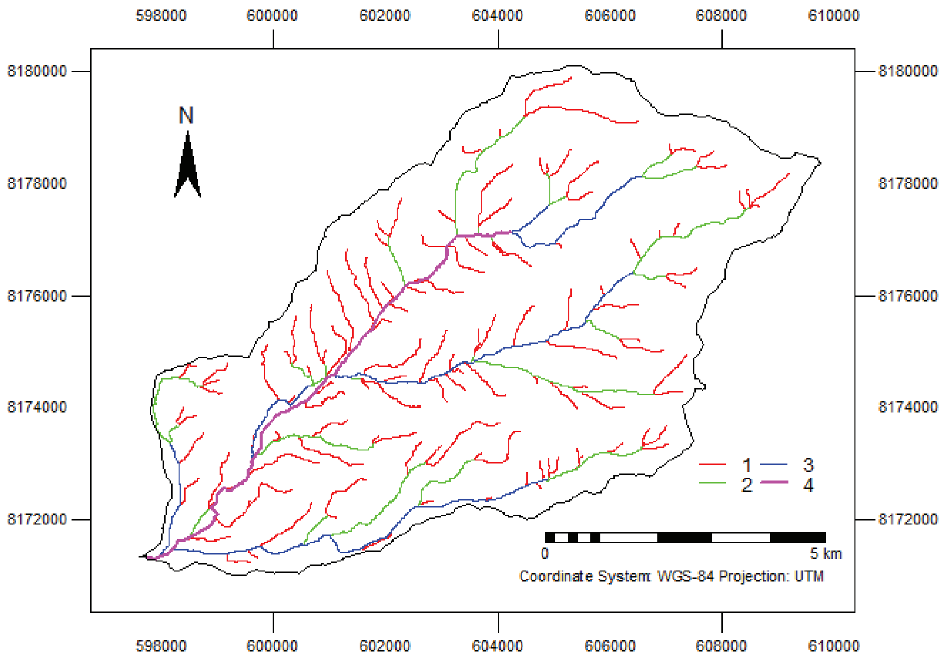

Figure 30 4th Strahler's stream order for the Achumani catchment (Aerial orthophoto restitution DEM)

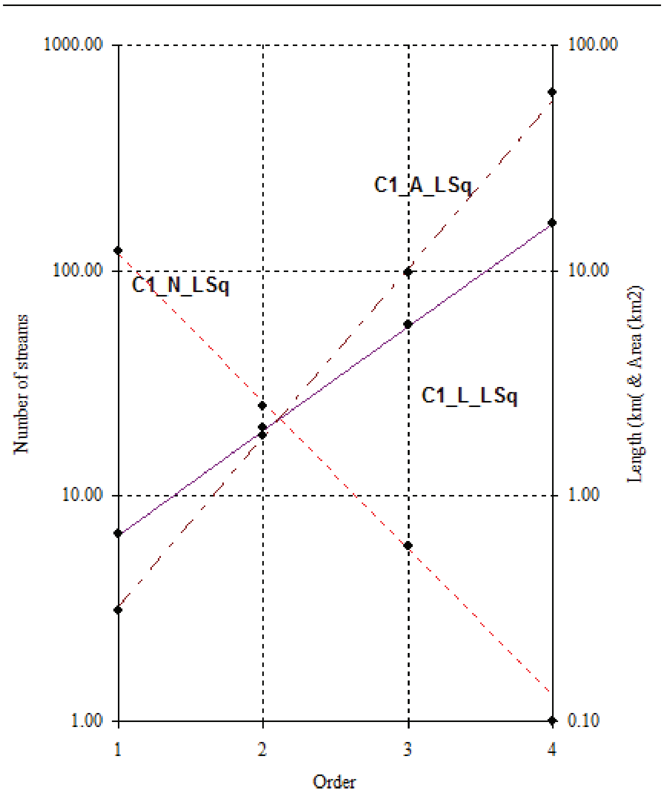

Figure 31 Horton statistics for Aerial orthophoto restitution DEM

Order	C1_N	C1_L	C1_A	C1_N_LSq	C1_L_LSq	C1_A_LSq
	(number)	(km)	(km2)	(number)	(km)	(km2)
1	122.00	0.68	0.31	118.83	0.67	0.33
2	25.00	1.86	2.01	26.35	1.93	1.82
3	6.00	5.72	9.73	5.84	5.61	10.22
4	1.00	16.09	61.40	1.30	16.27	57.23

Horton's Ratios		
Rb	Rl	Ra
4.87	2.89	5.72

Table 19 Horton statistics for Aerial orthophotos restitution DEM

4.7. Sensitivity analysis

Sensitivity analysis is used to determine how “sensitive” a model is to changes in the value of the parameters of the model and to changes in the structure of the model (Breierova and Choudhari, 1996). As it was mentioned before, the threshold stream value is one of the main variables that help to define the complexity of a catchment’s drainage system. To assess how the Horton’s ratios value (refer to Section 3.2.1) change depending on the threshold stream value, the following figures were made. It is important that the selected threshold stream value generates the same Strahler’s order as the final catchment network ordering map.

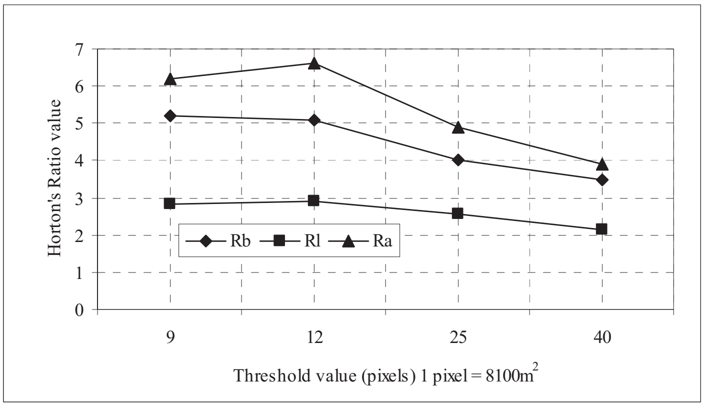

Figure 32 Sensitivity Analysis for SRTM DEM

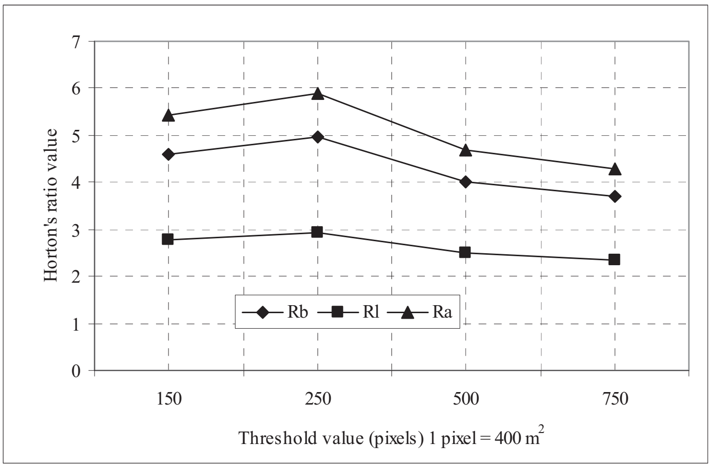

Figure 33 Sensitivity Analysis for Topographic map DEM

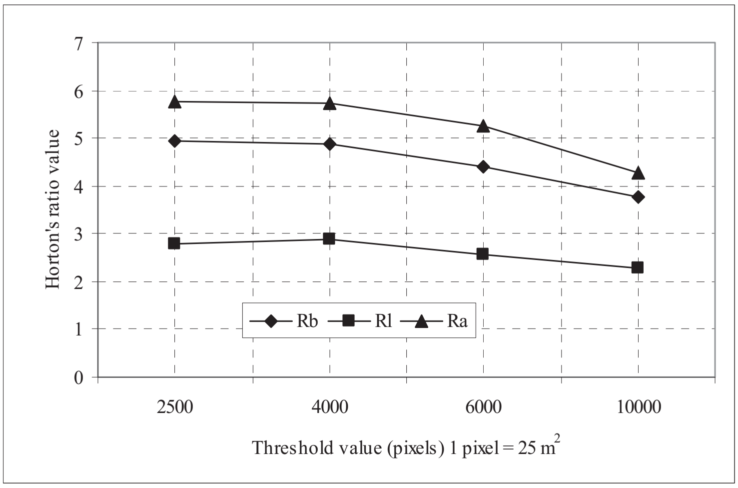

Figure 34 Sensitivity Analysis for Aerial orthophotos restitution DEM

Figure 32, Figure 33 and Figure 34 show the sensitivity analysis made for the SRTM, Topographic map and Aerial orthophotos restitution DEM respectively. In the three cases and in the particular case of the Achumani catchment, it can be seen that the threshold values chosen for the final catchment network ordering (12, 250, 4000 pixels respectively) produce the highest Horton's ratios values.

4.8. Model development

As it was explained in Section 3.1.3.3 three main type of input are required.

- The geomorphological parameters of the catchment (Horton's ratios)
- Effective rainfall
- Discharge measurements

4.8.1. Model input

4.8.2. Geomorphological parameters and Horton Statistics

Table 20**Error! Reference source not found.** shows the final results for the DEM Hydroprocessing explained in Section 0. Columns below the DEM Source title represent the three different DEM sources that were used in this thesis. SRTM (Shuttle Radar Topography Mission), TM (DEM obtained from Topographic maps) and AOR (DEM obtained from Aerial orthophotos restitution)

	DEM Source		
Geomorphological parameter	**SRTM**	**TM**	**AOR**
Order	4	4	4
Area	62.81	61.78	61.8
Length of the main stream (km)	8.55	10.68	10.37
Bifurcation ratio	5.07	4.95	4.87
Length ratio	2.89	2.94	2.89
Area ratio	6.6	6.1	6.05

Table 20 Geomorphological parameters for the three DEM sources

The difference among the Horton's statistics for every DEM source varies from 4% for the bifurcation ratio, 2% for the length ratio and 9% for the area ratio.

4.8.3. Effective rainfall and discharge data

In Section 4.4 it was explained the methodology to obtain the effective rainfall for the 4-5-Dec-1991 event. From this explanation it was concluded that two of the three chosen methods can be applicable to this event (the SCS effective rainfall and the Phi index). Table 21 shows the final input values for the modelling process. These two variables are the direct runoff hydrograph and the effective rainfall for both infiltration methods.

Time	Observed data		Effective rainfall		Direct runoff hydrogram
	Precipitation	Discharge	SCS method	Phi index	
Day-Hour	mm	m3/s	mm	mm	m3/s
4-9	0.0	0.15			
4-10	6.0	0.17	0.04	5.53	
4-11	0.0	0.17			
4-12	0.0	0.17			
4-13	0.0	0.17			
4-14	2.1	0.17	0.30	1.63	
4-15	0.1	1.64	0.02		1.47
4-16	0.2	0.9	0.04		0.73
4-17	0.0	0.532			0.362
4-18	0.0	0.4			0.23
4-19	1.5	1.8	0.40	1.03	1.63
4-20	0.2	2.08	0.06		1.91
4-21	0.2	2.41	0.06		2.24
4-22	0.1	2.33	0.03		2.16
4-23	0.3	1	0.10		0.83
5-0	0.2	1.18	0.07		1.01
5-1	0.1	1.1	0.03		0.93
5-2		1.23			1.06
5-3		1.07			0.9
5-4		0.48			0.31
5-5		0.55			0.38
5-6		0.77			0.6
5-7		0.643			0.473
5-8		0.643			0.473
5-9		0.56			0.39
5-10		0.48			0.31
5-11		0.4			0.23
5-12		0.3			0.13
5-13		0.3			0.13
5-14		0.29			0.12
5-15		0.29			0.12
5-16		0.28			0.11
5-17		0.27			0.1
5-18		0.27			0.1

Table 21 Effective rainfall and discharge input values

4.9. Basic steps for the modeling process

Shows the basic steps for the IUH calculation, for a detailed description of the equations a steps refer to Appendix 2

1. Horton statistics: Rb Bifurcation ratio Rl Length ratio, Ra Area ratio	Horton's Ratios		
	Rb	Rl	Ra
	5.07	2.89	6.6

2. Transition probabilities	p_{12}	p_{13}	p_{14}	p_{23}	p_{24}	p_{34}
	0.70	0.22	0.13	0.73	0.27	1.00

3. State probabilities	π_{r1}	π_{r2}	π_{r3}	π_{r4}
	0.45	0.27	0.24	0.04

4. Probability at a given path p(s)	p_{s1}	p_{s2}	p_{s3}	p_{s4}	p_{s5}	p_{s6}	p_{s7}	p_{s8}
	0.23	0.09	0.01	0.06	0.20	0.07	0.24	0.04

5. Estimation of KB	K_B	2.50
γ fitting parameter	γ	0.30

6. Mean holding time of a ith-order channel	$1/\lambda_{c1}$	$1/\lambda_{c2}$	$1/\lambda_{c3}$	$1/\lambda_{c4}$
	0.27	0.38	0.55	0.78

7. Mean holding time of a ith-order region	$1/\lambda_{r1}$	$1/\lambda_{r2}$	$1/\lambda_{r3}$	$1/\lambda_{r4}$
	0.17	0.36	0.13	0.03

8. Probability density function of travel time at each paths	$C_{j,k} = \dfrac{\lambda_{x_1} \ldots \lambda_{x_{k-1}}}{(\lambda_{x_1} - \lambda_{x_j}) \ldots (\lambda_{x_{j-1}} - \lambda_{x_j}) \cdot (\lambda_{x_{j+1}} - \lambda_{x_j}) \ldots (\lambda_{x_k} - \lambda_{x_j})}$
9. GIUH Convolution	$h(t) = \sum_{s \in S} \sum_{j=1}^{k} C_{j,k} \exp\left\{-\lambda_{x_j} t\right\} \cdot p(s)$ $s = (x_1, \ldots, x_k)$

Table 22 Basic steps for the GIUH modelling process

5. Results and discussion

5.1. Model output

5.2. Model performance according to DEM source

Based on Table 20 three different hydrographs were calculated, each one corresponding to a specific DEM source and using the effective rainfall based on the SCS methodology (Table 21).

As it can be seen in Figure 35 the model response to changes in the Horton's ratios is not significant. The instantaneous unit hydrographs shown in the figure belong to the three DEM sources that were chosen for the present study. On the right part of the figure the value difference among the Horton's ratios for every DEM source is also shown. This variation goes from 0.291 to 0.303 (hr^{-1}) which represents a variation of approximately 4%. It was also verified that this variation in the unit hydrograph does not affect significantly to the direct runoff hydrograph generated. Due to its little variation it can not be well graphically represented. The following sections will be developed using the SRTM DEM source.

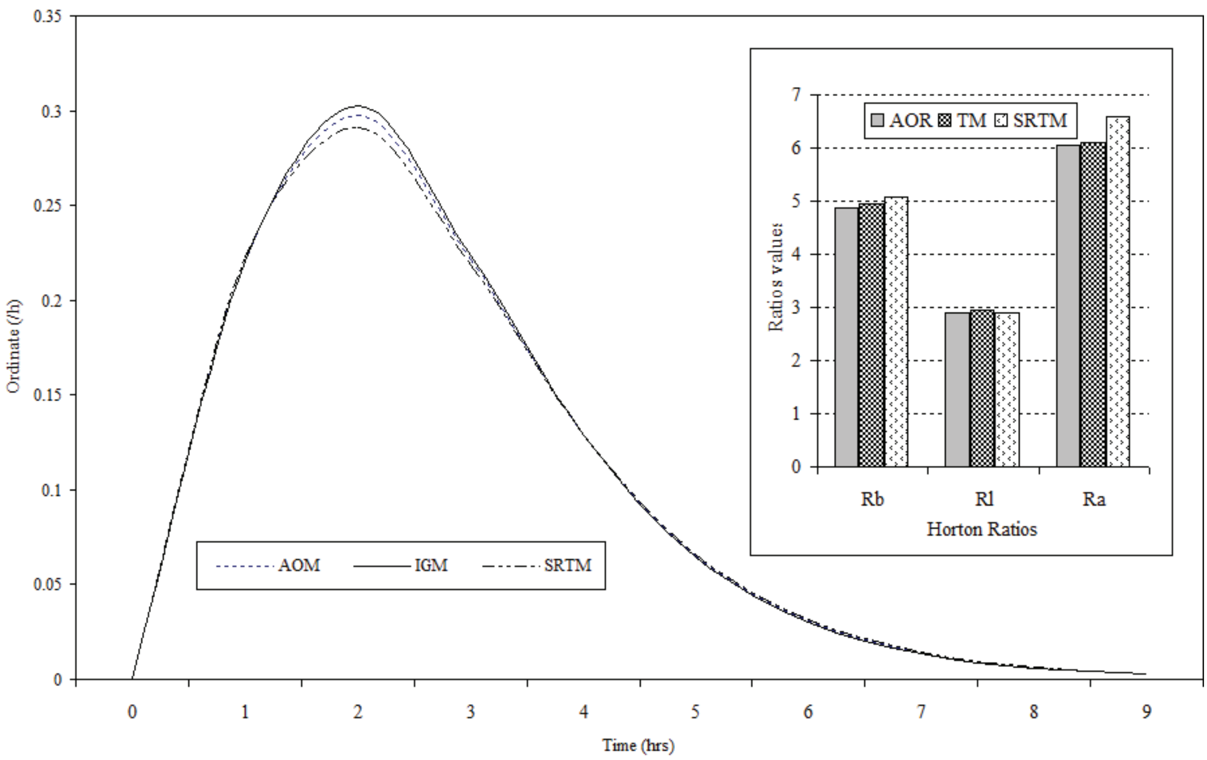

Figure 35 Model performance according to the DEM source

5.3. Direct runoff hydrograph using the SCS effective rainfall

Figure 36 shows the direct runoff hydrograph using the GIUH methodology (Refer to Section 4.9 or Appendix 2). The dotted line represents the hydrograph without any calibration process. It can be observed that it underestimates de measured peak discharge value. The calibration process is based on the K_B factor which represents the distance between the centre of gravity of the observed hydrograph and the hyetograph. A K_B value of 2.5 hours was determined to give the results shown in Figure 36 where the calibrated hydrograph estimates more reasonably the shape and the peak discharge valu of the measured hydrograph.

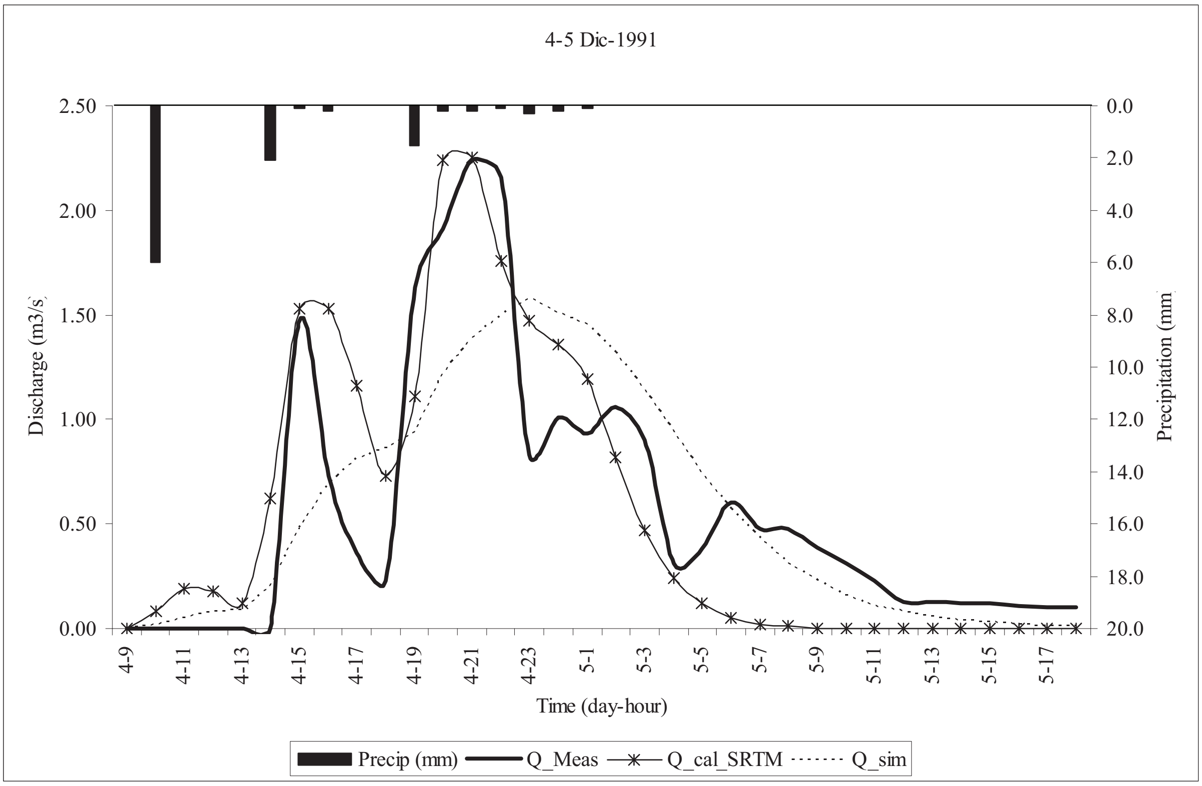

Figure 36 Direct runoff hydrograph based on the SRTM DEM and the SCS method

5.4. Direct runoff hydrograph using the Phi-index method

Using the hyetograph corresponding to the phi-index methodology and after the calibration process with a mean holding time K_B of 12 hours was made, the hydrograph shown in Figure 37 was defined. As it can be seen the predicted results could only make a good approximation to the peak value of the observed hydrograph. The main reason for this result is that the final phi-index hyetograph considered only one precipitation record for the whole event.

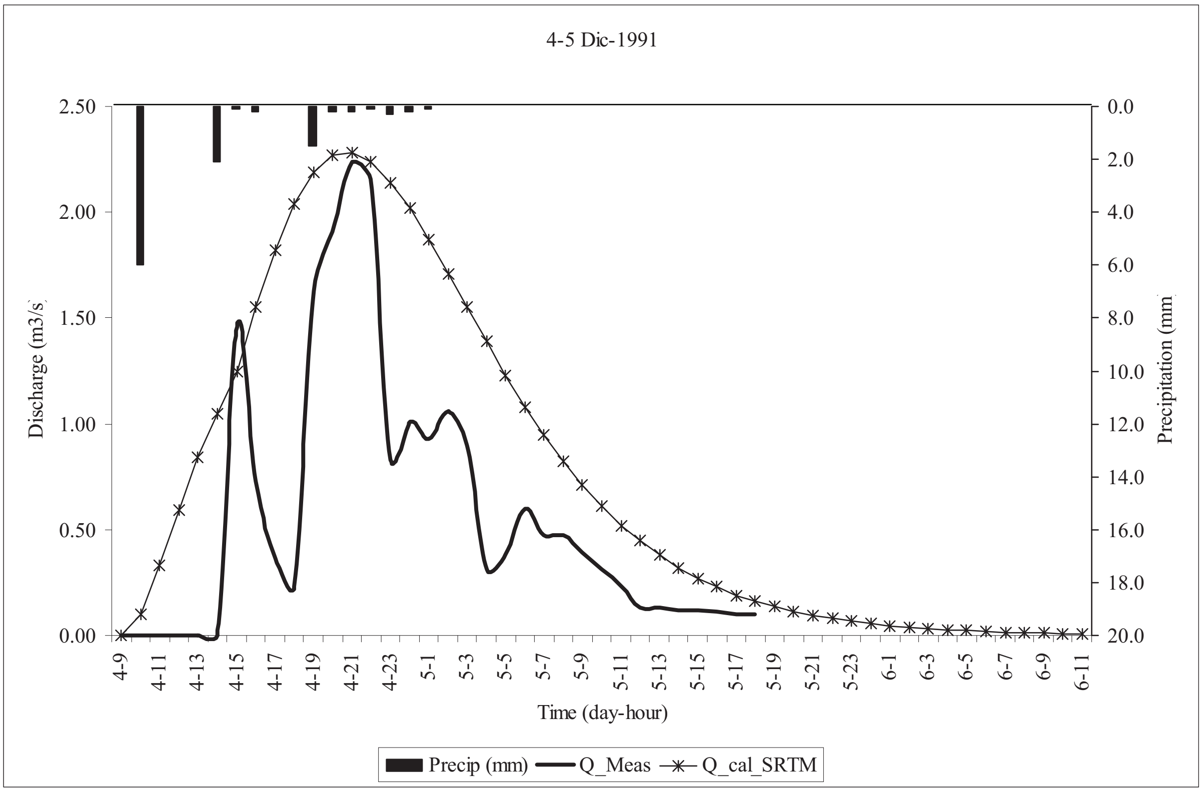

Figure 37 Direct runoff hydrograph based on the SRTM DEM and the Phi-index method

5.5. Statistical performance

In order to assess the statistical performance of the GIUH model, two statistical parameters were considered.

- The model efficiency
- The root mean square error

The Nash-Sutcliffe model efficiency coefficient is used to assess the predictive power of hydrological models. It is defined as:(Nash and Sutcliffe, 1970)

$$ME = 1 - \frac{\sum_{i=1}^{n}(O_i - P_i)^2}{\sum_{i=1}^{n}(O_i - O_a)^2} \quad \textbf{Eq. 14}$$

Where:

ME is the model efficiency

O_i is the observed value

P_i is the predicted value

O_a is the observed average

Applying this equation to the predictions using the SCS method and the observed discharge values showed in Figure 36 a ME=0.67 was found. Observing the calibrated hydrograph and the measured hydrograph, the peak value was matched with accuracy meanwhile the shape of both hydrographs at the recession period of the does not match properly.

The r-squared value can be interpreted as the proportion of the variance in the observed discharge values attributable to the variance in the simulated values.

$$r = \frac{\sum_{i=1}^{n}(P_i - P_a)\cdot(O_i - O_a)}{\sqrt{\sum_{i=1}^{n}(P_i - P_a)^2 \cdot \sum_{i=1}^{n}(O_i - O_a)^2}} \quad \textbf{Eq. 15}$$

Where:

r is the root mean square error

O_i is the observed value

P_i is the predicted value

O_a is the observed average

P_a is the predicted average

Applying this equation to the predictions using the SCS method and the observed discharge values a r^2=0.79 was found.

The statistical performance between the observed discharge values and the predictions using the Phi index, show a low performance, 0.14 and 0.69 for the model efficiency and the r squared respectively. The main reason for these results is the effective rainfall that was calculated with this method. (refer to Section 4.4.2)

5.6. Instantaneous unit hydrograph

Figure 38 show the instantaneous unit hydrograph calculated for the Achumani catchment. This unit hydrograph will be used to estimate the design discharge values for a return period of 100 years using the design hyetographs defined in Section 4.2. The direct runoff curve Q_n is calculated using the excess rainfall P_m and the unit hydrograph U_{n-m+1} (Chow V. et al., 1994).

$$Q_n = \sum_{m=1}^{n \le M} P_m \cdot U_{n-m+1} \quad \textbf{Eq. 16}$$

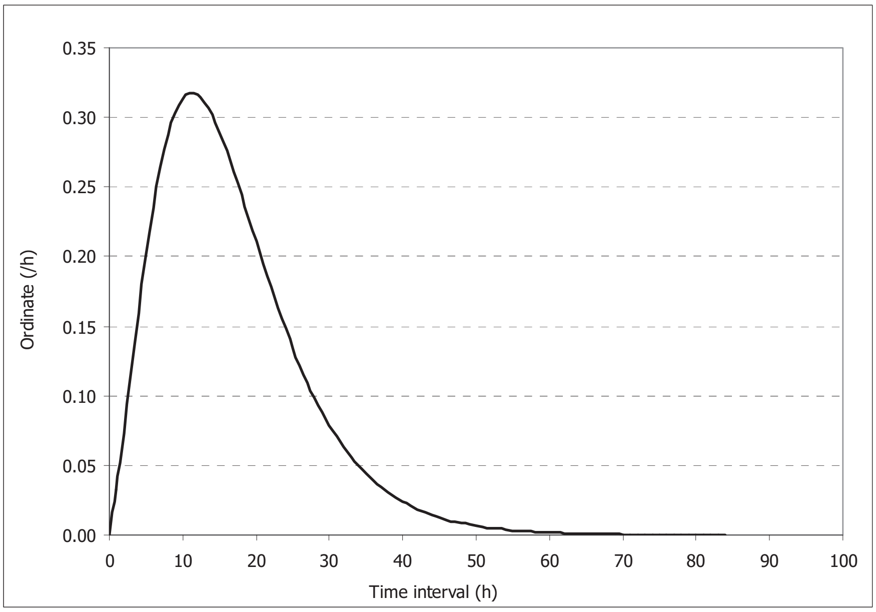

Figure 38 Instantaneous unit hydrograph for the Achumani catchment

5.7. Design discharge values for 50 and 100 years return period

The hydrographs presented in Figure 39 were calculated using the design hyetograph from Millipunku station IDF curves and the design hyetograph from San Calixto distribution coefficients. (Refer to Section 4.2)

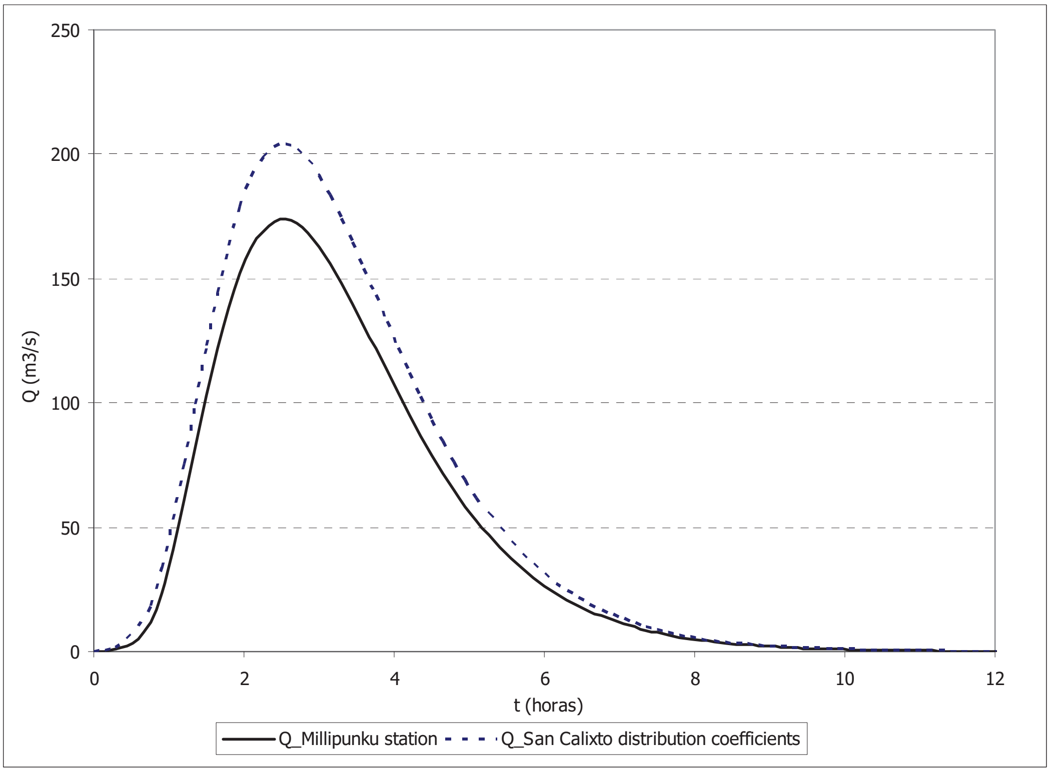

Figure 39 Design runoff hydrograph for a 100 years return period

The San Calixto distribution coefficients estimate a higher peak discharge value than the Millipunku station (204.0 m^3/s and 173.8 m^3/s respectively). This represents a variation of approximately 17%.

This same methodology was followed to determine the design discharge values for a 50 years return period. Table 23 shows the final results. As these values will be used for hydraulic structures design purposes, the discharge values obtained using the San Calixto distribution coefficients are advised to be used. These discharge values do not consider the sediment material transport, further research on this topic must be done in order to assess its effect on the obtained results. As it was described in Section 2.2.4, the type of soil and the erosion processes characteristics in the area affect the catchment hydrological response to rainfall.

	T=100 years	T=50 years
Millipunku	173.8	158.1
San Calixto	204.0	185.3

Table 23 Design discharge values (m^3/s)

As it was mentioned in Section 3.1.1, topographical survey and channel inspections were made in order to find watermarks from past rainfalls that will be used for calibration and validation purposes. Figure 40 shows a cross section located at the outlet of the Achumani catchment, during the channel inspection a watermark at 1.5 meters from the channel base was found. This watermark corresponds to the last rain period where according to San Calixto station, on January 29th a maximum precipitation of 40 mm was registered. Making the relation between this registered precipitation and the maximum precipitation for 24 hours presented in Table 7, it can be associated to a return period of 25 years for the Millipunku station. Following the same steps described in Section 4.2 the hyetograph for a return period of 25 years was found and using the instantaneous unit hydrohgraph a design discharge value of 164.3 m^3/s was estimated.

Cross section characteristics:

Water mark level = 1.5m

Base = 15m, Height= 2.7m

n Manning = 0.03 (river bed) (Chow, 1959)

slope S = 0.04

Using Manning's equation a discharge of 174.06 m^3/s is calculated

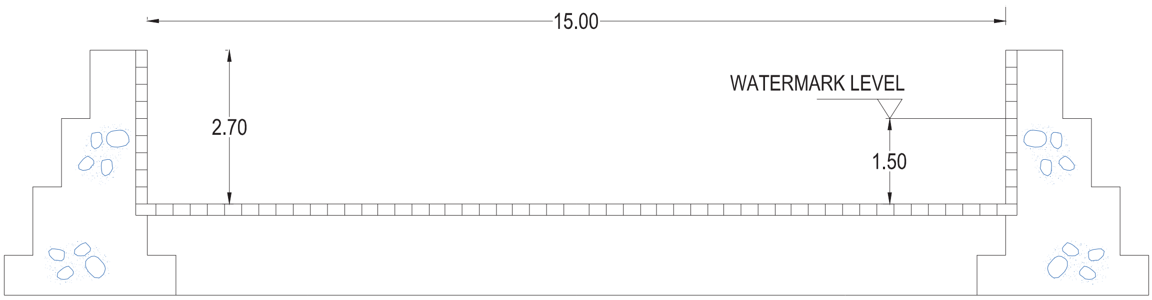

Figure 40 Cross section at the outlet of the Achumani catchment

The difference between these two calculations (174.03 m^3/s for the watermark level and 164.3 m^3/s for the estimated discharge using the GIUH) is around 9.76 m^3/s, equivalent to a 6%. This difference can be considered tolerable since small variations in the roughness value ‘n’ in Manning’s equation, affect significantly the discharge value.

6. Conclusions and Recommendations

6.1. Conclusions

This study has developed the GIUH to assess its performance for the Achumani catchment, to determine the influence of the DEM source over the drainage network definition and to estimate design discharge values for 50 and 100 years return period. Based on the study, the following conclusions can be made.

- According to the results obtained from the three DEM sources assessment, the DEM resolution does not affect significantly to the final network catchment ordering map and the Horton's statistics. The variation resulting from the Horton values is around 4%, 2% and 9% for the bifurcation ratio, length ratio and area ratio respectively. This DEM assessment process included the DEM hydro-processing and the threshold area definition based on the GCP of the main streams location in the Achumani catchment.
- Due to the lack of information for the Achumani catchment, the development of the GIUH methodology becomes a promising tool for hydrological purposes, especially for the frequency analysis necessary to define design discharge values. However, it is important to mention that more rainfall events are necessary to validate the K_B value and improve the IUH for the Achumani catchment.
- The design discharge values for 50 and 100 years return period presented in this study, become a good reference for hydraulic structures design along the main stream and outlet of the Achumani catchment.
- The use of the SRTM imagery, due to its public access and easy processing, is highly recommended to be used in similar studies for adjacent catchments in La Paz city, using the GIUH methodology developed in this thesis or with a DEM based hydrological model (e.g. TOPMODEL).
- The effective rainfall method developed by the SCS presented better results compared to Kostiakov's model or the Phi-index method. The elaboration of the land-cover map is a basic and important step to define the initial abstraction necessary for accurate effective rainfall estimation. Despite this good performance of the method, a more intensive study related to infiltration processes and soil characteristics must be done.
- The frequency analysis showed that the record period for the Millipunku station is unfortunately too short (1991-1994) to perform a reliable frequency analysis. The use of distribution coefficients developed for San Calixto station enabled to validate the design hyetograph since the variation between both of them is around 17%.

6.2. Recommendations

Although the GIUH model is found to perform with a reasonable accuracy in the Achumani catchment, the model efficiency and predictions can be improved considering the following

- The sediment transport analysis was not carried out in this study, only a brief explanation based on past studies was made. It is recommended to assess its effect on the hydrological process over the Achumani catchment due to the geomorphological and geological conditions described.
- The catchment instrumentation is a crucial factor for projects development. Unfortunately, since 2002 the Achumani catchment does not have any type of hydrological instrumentation. It is highly recommended that the authorities in charge (SENAMHI) make the much effort possible to install new pluviographic instruments in order to get a continuous rainfall registration.
- A subcatchment division can be performed to the Achumani catchment in order to obtain discharge values for different streams. Working at this level, the assumption of uniform rainfall over the study area can be accepted. This issue may become important in order to develop projects related to sediment retention structures or small channel projects.
- It is recommended to develop new studies for the Achumani catchment in order to assess RS techniques as a tool for meteorological data collection. (e.g. the use of METEOSAT, MODIS imagery, ASTER DEM extraction, etc)

References

Bhadra, A. et al., 2008. Development of a geomorphological instantaneous unit hydrograph model for scantily gauged watersheds. Environmental Modelling & Software, 23(8): 1013-1025.

Breierova, L. and Choudhari, M., 1996. An Introduction to Sensitivity Analysis. Massachusetts Institute of Technology, pp. 41-107.

Cleveland, T.G., He, X., Fang, X. and Thompson, D.B., 2007. Synthesis of Unit Hydrographs from Digital Elevation Models, pp. 15.

Chow V., D. R. Maidment and Mays, L.W., 1994. Applied Hydrology. Mc Graw Hill, 580 pp.

Chow, V.T., 1959. Open-Channel Hydraulics. McGraw-Hill Inc.

Feller, W., 1971. An Introduction to Probability Theory and Its Applications, 2. John Wiley, New York.

Ferrer M., Blanco J. and J., R., 2006. Methodological proposal for the adaptation of the curve number parameter with new data sources, III Conference of Civil Engineering, territory and environment, Zaragoza (Spain).

Fleurant, C., Kartiwa, B. and Roland, B., 2006. Analytical model for a geomorphological instantaneous unit hydrograph. Hydrological Processes, 20(18): 3879-3895.

Gupta, V.K., Waymire, E. and Wang, C.T., 1980. A Representation of an Instantaneous unit Hydrograph from Geomorphology. Water Resources Research, 16(5): 855-862.

Jain, V. and Sinha, R., 2003. Derivation of Unit Hydrograph from GIUH Analysis for a Himalayan River. Water Resources Management, 17: 355-375.

Karvonen, T., Koivusalo, H., Jauhiainen, M., Palko, J. and Weppling, K., 1999. A hydrological model for predicting runoff from different land use areas. Journal of Hydrology, 217(3-4): 253-265.

Kostiakov, A.N., 1932. On the dynamics of the coefficient of water-percolation in soils and on the necessity of studying it from a dynamic point of view for purposes of amelioration Transactions of 6th Congress of International Soil Science Society Moscow: Part A 17-21.

Kumar, R., Chatterjee, C., Singh, R.D., Lohani, A.K. and Kumar, S., 2007. Runoff estimation for an ungauged catchment using geomorphological instantaneous unit hydrograph (GIUH) models. Hydrological Processes, 21(14): 1829-1840.

Maathuis B.H.P. and Wang L., 2006. Digital Elevation Model Based Hydro-processing. Geocarto International, 21(1): 21-26.

Mendoza, J.C., 2000. Intensity-Duration-Frequency curves for La Paz City, Water Science Specialized magazine. Hydrology and Hydraulics Institute UMSA, La Paz - Bolivia, pp. 14.

Mezencev, V.J., 1948. Theory of formation of the surface runoff. Meteorologiae Hidrologia, 3: 33-40.

Nania, L., 2002. The catchment and the hydrological processes. Granada University, Granada - Spain, pp. 62.

Nash, J.E. and Sutcliffe, J.V., 1970. River flow forecasting through conceptual models part I -- A discussion of principles. Journal of Hydrology, 10(3): 282-290.

Nguyen Hong, Q., 2006. Rainfall runoff modeling in the ungauged Can Le catchment, Saigon river basin, ITC, Enschede, 92 pp.

Noorbakhsh, M.E., Rahnama, M.B. and Montazeri, S., 2005. Estimation of Instantaneous Unit Hydrograph with Clark's Method Using GIS Techniques. Journal of Applied Sciences, 5(3): 455-458.

Patil, J.P., Sarangi, A., Singh, A.K. and Ahmad, T., 2008. Evaluation of modified CN methods for watershed runoff estimation using a GIS-based interface. Biosystems Engineering, 100(1): 137-146.

PCA Consulting Engineers and NIPPON KOEI CO. LTD., 2007. Review and update of the drainage master plan for the urban area of La Paz City. Municipal Government of La Paz City, La Paz.

Porta J., Lopez M. and Roquero C., 1999. Edafology for agriculture and enviornment. Madrid Mundi Prensa, 849 pp.

Reuter H.I, A. Nelson and A. Jarvis, 2007. An evaluation of void filling interpolation methods for SRTM data. International Journal of Geographic Information Science, 21(9): 983-1008.

Rodriguez-Iturbe, I. and Valdes, J.B., 1979. The Geomorphologic Structure of Hydrologic Response. Water Resources Research, 15(6): 1409-1420.
Sarangi, A., Singh, D.K. and Singh, A.K., 2008. Evaluation of curve number and geomorphology-based models for surface runoff prediction from ungauged watersheds. Current Science, 94(12): 1620-1626.
Shadeed, S., Shaheen, H. and Jayyousi, A., 2007. GIS-based KW-GIUH hydrological model of semiarid catchments: The case of Faria catchment, Palestine.
Shaheen, H., Jayyousi, A., Shadeed, S. and Jarrar, A., 2005. Hydrograph estimation in semiarid regions using GIS supported GIUH model. Ninth International Water Technology Conference: 371-380.
Strahler, A.N., 1957. Quantitative analysis of watershed geomorphology. Transactions American Geophysical Union, 38: 913-920.
Turner, E., 2006. Comparison of infiltration equations and their field validation by rainfall simulation, University of Maryland, College Park, 202 pp.

Appendices

APPENDIX 1 LIST OF ACRONYMS

GIUH	Geomorphological Instantaneous Unit Hydrograph
GIS	Geographic Information System
RS	Remote Sensing
DEM	Digital Eloevation Model
SENAMHI	Meteorological and Hydrologycal National Service
UH	Unit Hydrograh
m.a.s.l.	Meters above sea level
IGM	Geographic Military Institute
GCP	Groun Control Point
GPS	Global Positioning System
SRTM	Shuttle Radar Topography Mission
IDF	Intensity Duration Frequency
PDF	Precipitation Duration Frequency
Ra	Horton's area ratio
Rb	Horton's bifurcation ratio
Rl	Horton's length ratio
DRH	Direct Runoff Hydrograph
ASCII	American Standard Code for Information Interchange
SCS	Soil Conservation Service

APPENDIX 2 A representation of an instantaneous unit hydrograph from geomorphology[2]

The fundamental idea on which this approach is based can be explained as follows. Suppose that a large number, say, n, of noninteracting water particles (thinking somewhat formally) are instantaneously injected in to a basin. Further suppose that each particle stays in the basin for a random amount of time T_B^i, $1 \leq i \leq n$, called its holding time. The holding times are independent and identically distributed (as T_B), because the water particles are assumed to be noninteracting and identical. Then in view of the 'lumped' equation of continuity, applied to the whole basin, and the law of large numbers [Feller, 1971] it follows that the iuh of the basin is equal to the probability density function (pdf) of T_B, as will be shown. The equivalence between the iuh and the pdf of T_B constitutes the basic idea on which this probabilistic approach is based (also see Rodriguez-Iturbe and Valdez [1979]).

In a natural basin a water particle injected randomly over the basin will follow a certain path through the 'overland' catchment regions and the channels before arriving at the basin outlet. The path function probability, that is, the probability that the particle follows a certain path, from among all possible paths, is quantified on the basis of the Strahler scheme for ordering the channel network in a basin. Each path has its own random holding time. The pdf of the basin holding time (i.e., the iuh) is obtained by first determining the probability that a particle follows a certain path, amongst all possible paths, to get to the outlet, multiplying it with the pdf of the random holding time for this path and then summing these products over all possible paths. This leads to a general mathematical representation of the iuh of a basin in terms of the basin geomorphology.

BRIEF REVIEW OF PERTINENT GEOMORPHOLOGY

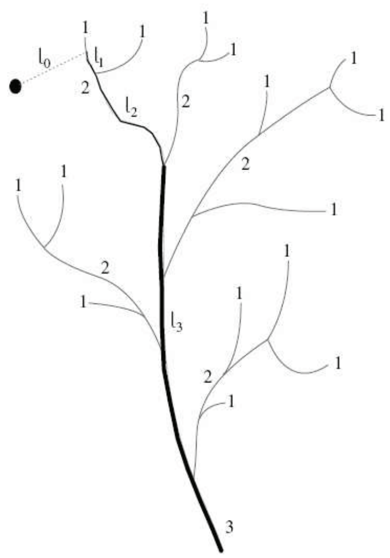

Figure 1 Strahler's stream order classification

Figure 1 shows a hypothetical watershed with the Strahler ordering procedure:

1) Channels that originate at a source are defined to be first-order streams

2) When two streams of order Ω join, a stream of order Ω + 1 is created

3) When two stream of different order join, the channel segment immediately downstream has the higher of the order of the two combining streams.(Rodriguez-Iturbe and Valdes, 1979).

The Horton Statistics operation calculates for each (Strahler) stream order number and for each merged catchment the (area ratio (R_A), bifurcation ratio (R_B), length ratio (R_L).

[2] Text extracted from Gupta (1980)

Bifurcation	$R_B = \dfrac{N_i}{N_{i+1}}$	where N_i and Ni+1 represent the number of streams in order i and i+1. Let ω represent the highest stream order in watershed, i = 1, 2,…, ω
Length	$R_L = \dfrac{L_{i+1}}{L_i}$	Li is the average length of channels of order i $L_i = \dfrac{1}{N_i}\sum_{j=1}^{N_i} L_j$
Area	$R_A = \dfrac{A_{i+1}}{A_i}$	Ai is the mean area of the contributing subcatchment to streams of order i, $A_i = \dfrac{1}{N_i}\sum_{j=1}^{N_i} A_j$ where Aj represents the total area that drains into the jth stream of order i

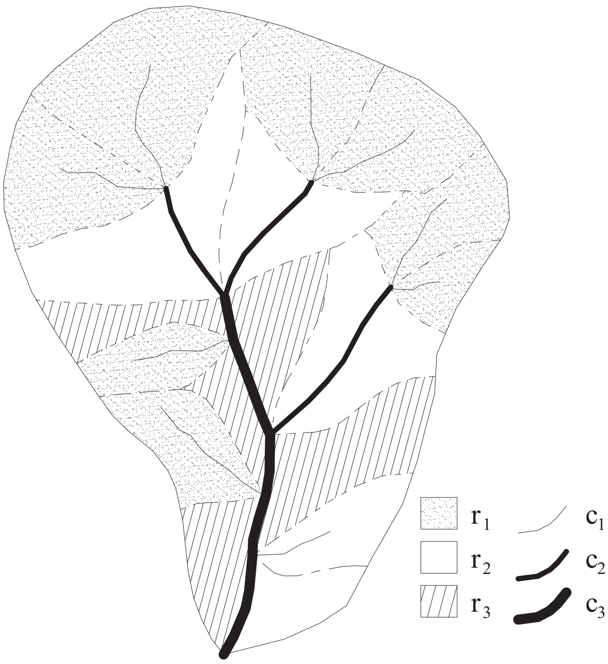

Figure 2 Third-order basin with Strahler's ordering system

In the ensuing developments we will generically use the symbol c_i to denote a channel state of Strahler order i, that is, an ensemble of all the channels of order i. Similarly r_i denotes an overland region state of Strahler order i, that is, an ensemble of the overland flow areas and/or creeks smaller than the first-order channels defined above, which flow directly into the channels of order i.

Ω denotes the order of a basin; c_i 1≤ i≤Ω, denotes a channel state of order i; and r_i 1≤ i≤Ω, denotes an overland region state of the basin. We assume on physical grounds that initially the particles will only be located in one of the overland regions r. so that the amount of rainfall that initially falls into the channels c_i 1≤ i≤Ω, is neglected. Since the n particles have been assumed to be weakly interacting, it is enough to consider the law of evolution of only one of these particles. Given that a particle is found in any one of the regions ri, it undergoes transitions according to the following rules:

Rule 1. The only possible transitions out of the state r_i are those of the form $r_i \rightarrow c_i$ 1≤ i≤Ω

Rule 2. The only possible transitions out of the state c_i are those of the form $c_i \rightarrow c_j$ for some j>i, i = 1, 2, ..., Ω.

Rule 3. Define a state c_Ω+1 as a trapping state c_i, that is, transitions out of the state c_Ω+1 are impossible.

The reader may observe that the rules 1-3 define a collection S = {s} of paths s which a particle may follow through to the trapping state, that is, the outlet of the basin. As an example, consider the forth-order network shown in Figure 2. The 'path space' S = {s_1, s_2, s_3, s_4} consists of the following four paths:

Path s_1 $r_1 \rightarrow c_1 \rightarrow c_2 \rightarrow c_3 \rightarrow c_4$

Path s_2 $r_1 \rightarrow c_1 \rightarrow c_3 \rightarrow c_4$

Path s_3 $r_2 \rightarrow c_2 \rightarrow c_3 \rightarrow c_4$

Path s_4 $r_3 \rightarrow c_3 \rightarrow c_4$

The above rules only specify the spatial evolution of a particle through a geomorphic network of channels and surface regions.

We now define the following quantities which can be calculated from an ordered channel network

π_{ri} is the ratio of the area of ri to the total area of the basin

$p_{ci,cj}$ is the proportion of channels of order i which merge into a channel of order j, $1<j\leq\Omega$

$p_{c\Omega,c\Omega+1}=1$

$p_{ri,ci}=1$

For a path $s\in S$ of the form $s = (x_1,\dots, x_k)$, where $x_1,\dots x_k \in \{c_1,\dots,c_\Omega, r_1,\dots,r_\Omega)$ define

$$p(s) = \pi_{x_1} \cdot p_{x_{11},x_2} \cdot \ldots \cdot p_{x_{k-1},x_k} \quad \textbf{(1)}$$

In addition, if Ts denotes the time to travel through the path s, then

$$T_s = T_{x_1} + T_{x_2} + \ldots + T_{x_k} \quad \textbf{(2)}$$

Let f_x denote the pdf of T_x and F_x is cumulative distribution function. Since T_B denotes the random time which a particle spends in the basin, then on the basis of the above consideration it can be expressed as

$$T_B = \sum_{s\in S} T_s I_s \quad \textbf{(3)}$$

Where $I_s=1$ if the particle follows the path s and Is=0 otherwise.

$$P(T_B < t) = \sum_{s\in S} P(T_s < t)\cdot p(s)$$
$$= \sum_{s\in S} F_{x_1} * F_{x_2} * \ldots * F_{x_k}(t)\cdot p(s) \quad \textbf{(4)}$$
$$s = (x_1,\ldots, x_k)$$

Where the asterisks denote the convolution operation. Differentiation of previous equation gives an explicit representation for the iuh.

$$h(t) = \sum_{s\in S} f_{x_1} * \ldots * f_{x_k}(t)\cdot p(s)$$
$$s = (x_1,\ldots, x_k) \quad \textbf{(5)}$$

Since particles move independently of one another and since the total flow at time t consists of the contribution from all the particles that were injected between times 0 and t, it follows that

$$Q_B(t) = \int_0^t h(t-u)i(u)du \quad \textbf{(6)}$$

In the representation of the iuh, the path probability functions p(s) can be completely specified on the basis of the basin geomorphology. However the pdf f_{xi} of the random holding times cannot be entirely determined from the geomorphic considerations. A. physically meaningful solution to this problem requires that the stochastic evolution of these particles be specified from dynamical considerations.

We assume that the pdf f_{xi} is exponential with some parameter $\lambda_{xi}>0$ then $f_{x1}*\ldots*f_{xk}$ becomes the k-fold convolution of independent but nonidentically distributed random variables. This can be expressed in the form

$$f_{x_1}*\ldots*f_{x_k}(t)=\sum_{j=1}^{k}C_{j,k}\exp\{-\lambda_{x_j}t\} \quad \textbf{(7)}$$

Where $C_{j,k}$ are given by Feller

$$C_{j,k}=\frac{\lambda_{x_1}\ldots\lambda_{x_{k-1}}}{(\lambda_{x_1}-\lambda_{x_j})\ldots(\lambda_{x_{j-1}}-\lambda_{x_j})\cdot(\lambda_{x_{j+1}}-\lambda_{x_j})\ldots(\lambda_{x_k}-\lambda_{x_j})} \quad \textbf{(8)}$$

So in this case the iuh is given by:

$$h(t)=\sum_{s\in S}\sum_{j=1}^{k}C_{j,k}\exp\left\{-\lambda_{x_j}t\right\}\cdot p(s) \quad \textbf{(9)}$$

$$s=(x_1,\ldots,x_k)$$

The expression above contains λ_{xi}, π_{ri}, $p_{ck,cj}$ $1\leq i\leq\Omega$, $1\leq k<j\leq\Omega$ as the unknown parameters. Since the path probability function p(s) appearing in (9) is completely specified in terms of the π_{ri}, $p_{ck,cj}$. A numerical evaluation of these parameters from geomorphologic considerations is now discussed.

Rodriguez-Iturbe found a physical specification for π_{ri}, $p_{ck,cj}$

$$p_{c_i,c_j}=\left\{(N_i-2N_{i+1})E[j,\Omega]\Big/\sum_{k=j}^{\Omega}E[k,\Omega]N_i\right\}+2(N_{i+1}/N_i)\delta_{i+1,j} \quad \textbf{(10)}$$

$$1\leq i<j\leq\Omega$$

Where δi+1j=1 if j=i+1 and 0 otherwise. The expressions for E[i,Ω] denoting the mean number of channels of order I, in a finite network of order Ω is given by:

$$E[i,\Omega]=N_i\prod_{j=2}^{i}[(N_{j-1}-1)/2N_j-1] \quad \textbf{(11)}$$

$$i=2,\ldots,\Omega$$

The probabilities π_{ri} i=1,2,…Ω can be expressed as

$$\pi_{r_1}=N_1\overline{A}_1/A_\Omega$$

$$\pi_{r_i}=\frac{N_i}{A_\Omega}\left[\overline{A}_i-\sum_{j=1}^{i-1}\overline{A}_j(N_jp_{ji}/N_i)\right] \quad \textbf{(12)}$$

$$i=2,\ldots,\Omega$$

Assume that the mean holding time $1/\lambda_c$, of an ith-order Strahler channel (state) is given by

$$1/\lambda_{c_i} = \gamma \overline{L_i}^{1/3} \quad \textbf{(13)}$$

$$1 \le i \le \Omega$$

Where λ is an empirical constant. Similarly, assume that the mean holding time 1/λ, of an ith-order overland region (state) is given by

$$1/\lambda_{r_i} = \gamma[\pi_{r_i} A_\Omega / 2N_i \overline{L}_i]^{1/3} \quad \textbf{(14)}$$

$$1 \le i \le \Omega$$

Physically speaking, both equations state that the mean holding time of a given state xi ∈ {c_i, ..., c_Ω, r_i, …, r_Ω} is proportional to some 'characteristic length' of that state.

In order to obtain the unknown parameter γ we observe that KB, the first moment of the iuh h(t), defined by

$$K_B = \int_0^\infty t \cdot h(t) \cdot dt \quad \textbf{(15)}$$

Is equal to the mean holding time of the basin, defined by

$$K_B = \left[\int_0^\infty t \cdot Q_B(t) \cdot dt \Big/ \int_0^\infty Q_B(t) \cdot dt \right] - [t_d / 2] \quad \textbf{(16)}$$

Where $t_d<\infty$ denotes the rainfall duration. However, from (15) and (16) it can be easily verified that

$$K_B = \sum p(s) \left[\frac{1}{\lambda_{x_1}} + \ldots + \frac{1}{\lambda_{x_k}} \right] \quad \textbf{(17)}$$

$$s = (x_1, \ldots, x_x)$$

The only unknown parameter on the right-hand side is γ, as is clear from the discussion above. Therefore once K_B is estimated (for a gaged basin) using (16) γ can be computed from (17). This determines all the parameters appearing in the expression for the iuh given by (9). For the present γ is considered a fitting parameter, since its physical interpretation, coming from (13) and (14), has not been obtained yet. However, such an interpretation is required for an application of this approach to ungauged basins.

EXAMPLE DEVELOPED FOR A 4TH ORDER CATCHMENT

The 'path space' for a forth order catchment S = {s_1, s_2, s_3, s_4,s_5, s_6, s_7, s_8} consists of the following eight paths:

Path s_1 $r_1 \rightarrow c_1 \rightarrow c_2 \rightarrow c_3 \rightarrow c_4$

Path s_2 $r_1 \rightarrow c_1 \rightarrow c_2 \rightarrow c_4$

Path s_3 $r_1 \rightarrow c_1 \rightarrow c_3 \rightarrow c_4$

Path s_4 $r_1 \rightarrow c_1 \rightarrow c_4$

Path s_5 $r_2 \rightarrow c_2 \rightarrow c_3 \rightarrow c_4$

Path s_6 $r_2 \rightarrow c_2 \rightarrow c_4$

Path s_7 $r_3 \rightarrow c_3 \rightarrow c_4$

Path s_8 $r_4 \rightarrow c_4$

The following table shows the values for the number of streams, the length, and area for every stream order. This process was made using the DEM-hydro processing module in ILWIS and applied to the SRTM image used for the present study The last three columns belong to the least square fit that was made.

Order	C1_N	C1_L	C1_A	C1_N_LSq	C1_L_LSq	C1_A_LSq
	(number)	(km)	(km2)	(number)	(km)	(km2)
1	103.00	0.70	0.34	104.16	0.73	0.35
2	21.00	2.26	2.46	20.53	2.10	2.31
3	4.00	5.84	14.80	4.05	6.06	15.26
4	1.00	14.38	62.73	0.80	17.51	100.70

For the present study the Horton’s ratios values that were calculated are:

$$R_B = \frac{N_i}{N_{i+1}} = \frac{104.16}{20.53} = 5.07$$

$$R_L = \frac{L_{i+1}}{L_i} = \frac{2.10}{0.73} = 2.89$$

$$R_A = \frac{A_{i+1}}{A_i} = \frac{2.31}{0.35} = 6.6$$

	DEM Source		
Geomorphological parameter	SRTM	TM	AOR
Order	4	4	4
Area	62.81	61.78	61.8
Length of the main stream (km)	8.55	10.68	10.37
Bifurcation ratio	5.07	4.95	4.87
Length ratio	2.89	2.94	2.89
Area ratio	6.6	6.1	6.05

Calculating the initial state probabilities for a 4th order catchment using (10) and (12), the expressions are:

$$\pi_{r_1} = \frac{R_B^3}{R_A^3}$$

$$\pi_{r_2} = \frac{R_B^2}{R_A^2}\left(1-\frac{R_B}{R_A}\left(\frac{2}{R_B}+\frac{(2R_B-1)(R_B^2-2R_B)}{R_B^2(2R_B-1)+R_B(R_B^2-1)+(R_B^2-1)(R_B-1)}\right)\right)=\frac{R_B^2}{R_A^2}\left(1-\frac{R_B}{R_A}p_{12}\right)$$

$$\pi_{r_3} = \frac{R_B}{R_A}\left(1-\frac{R_B^2}{R_A^2}p_{13}-\frac{R_B}{R_A}p_{23}\right)$$

$$\pi r_4 = 1-\left(\frac{R_B}{R_A}\right)^3 p_{14}-\left(\frac{R_B}{R_A}\right)^2 p_{24}-\left(\frac{R_B}{R_A}\right)p_{34}$$

$$p_{12} = \frac{2}{R_B}+\frac{(2R_B-1)(R_B^2-2R_B)}{R_B^2(2R_B-1)+R_B(R_B^2-1)+(R_B^2-1)(R_B-1)}$$

$$p_{13} = \frac{(R_B^2-1)(R_B-1)}{R_B^2(2R_B-1)+R_B(R_B^2-1)+(R_B^2-1)(R_B-1)}$$

$$p_{14} = \frac{(R_B^2-1)(R_B-1)(R_B-2)}{R_B^3(2R_B-1)+R_B^2(R_B^2-1)+R_B(R_B^2-1)(R_B-1)}$$

$$p_{23} = \frac{R_B-2}{2R_B-1}+\frac{2}{R_B}$$

$$p_{24} = \frac{R_B-1}{R_B(2R_B-1)}(R_B-2)$$

$$p_{34} = 1$$

Applying the equations for the initial state and transition probabilities (π_{xi} and $p_{xi,xj}$) as well as the path probabilities p(s).

For Ra=6.6 and Rb=5.07

p_{12}	p_{13}	p_{14}	p_{23}	p_{24}	p_{34}
0.703	0.218	0.132	0.730	0.270	1.000

π_{r1}	π_{r2}	π_{r3}	π_{r4}
0.453	0.271	0.238	0.037

The path probability is defined by (1) and according to all the possible paths fro a 4th order catchment we have

$$p(s1) = \pi_{r_1} \cdot p_{12} \cdot p_{23} \cdot p_{34}$$
$$p(s2) = \pi_{r_1} \cdot p_{12} \cdot p_{24}$$
$$p(s3) = \pi_{r_1} \cdot p_{13} \cdot p_{34}$$
$$p(s4) = \pi_{r_1} \cdot p_{14}$$
$$p(s5) = \pi_{r_2} \cdot p_{23} \cdot p_{34}$$
$$p(s6) = \pi_{r_2} \cdot p_{24}$$
$$p(s7) = \pi_{r_3} \cdot p_{34}$$
$$p(s8) = \pi_{r_4} \cdot p_{34}$$

Applying these formulas to the initial state and transition probabilities.

p_{s1}	p_{s2}	p_{s3}	p_{s4}	p_{s5}	p_{s6}	p_{s7}	p_{s8}
0.233	0.086	0.013	0.060	0.198	0.073	0.238	0.037

The next step is estimate de K_B parameter; this can be made estimating the distance between the centre of gravity of the design hyetograph and the runoff hydrograph

$$K_B = \sum p(s) \cdot \gamma \cdot \left[\frac{1}{\lambda_{r_1}} + \ldots + \frac{1}{\lambda_{r_\Omega}} + \frac{1}{\lambda_{c_1}} + \ldots + \frac{1}{\lambda_{c_\Omega}} \right]$$
$$s = (x_1, \ldots, x_x)$$

For an estimated K_B equal to 12 hr (This value may vary according to the calibration process)

$$\gamma = \frac{K_B}{\sum p(s) \cdot \left[\frac{1}{\lambda_{r_1}} + \ldots + \frac{1}{\lambda_{r_\Omega}} + \frac{1}{\lambda_{c_1}} + \ldots + \frac{1}{\lambda_{c_\Omega}} \right]}$$
$$s = (x_1, \ldots, x_x)$$

Calculating every $1/\lambda_{ri}$ and $1/\lambda_{ci}$ using (13) and (14).

$1/\lambda_{c1}$	$1/\lambda_{c2}$	$1/\lambda_{c3}$	$1/\lambda_{c4}$
0.27	0.38	0.55	0.78

$1/\lambda_{r1}$	$1/\lambda_{r2}$	$1/\lambda_{r3}$	$1/\lambda_{r4}$
0.17	0.36	0.13	0.03

Applying (8) and (9) using these values, the probability density function defined by Feller is calculated.

At this step a spreadsheet is necessary because it has to be calculated for every time step.

APPENDIX 3 Effective Rainfall calculation according to the SCS methodology

The Curve Number Method was originally developed by the Soil Conservation Service for conditions prevailing in the United States. Since then, it has been adapted to conditions in other parts of the world. Although some regional research centres have developed additional criteria, the basic concept is still widely used all over the world.

Effective rainfall is the component of the storm hyetograph which is neither retained on the land surface nor which infiltrates into the soil. The effective rainfall produces overland flow that results in the direct runoff hydrograph from a sub-area of a catchment. (Chow V. et al., 1994)

The effective rainfall is expressed by:

$$P_n = \frac{(P - P_0)^2}{P + 4P_0}$$

Where:

P = Total precipitation registered

P_n = Effective rainfall

P_0 = Initial abstraction

The initial accumulation of rainfall or the called initial abstraction represents interception, depression storage, and infiltration before the start of runoff. After runoff has started, some of the additional rainfall is lost, mainly in the form of infiltration; this is called actual retention. With increasing rainfall, the actual retention also increases up to some maximum value: the potential maximum retention which is directly related to the initial abstraction. (Chow V. et al., 1994).

These P_0 values (that now on will be named as P_0(II)) suppose a certain degree of soil moisture (AMC). If the previous days to the rainfall there have been significant rainfall, then the abstractions (surface retention, infiltration, etc.) will be lower, thus the real value of P_0 will be lower. By the other hand, if the previous days were out of rainfall, the soil will be dry and all the abstractions will be higher, thus the P_0 will get a higher value.

The following equations describe the relations among the three different AMC (Antecedent Moisture Condition).

Dry previous days $\quad P_0(I) = 2.38 \cdot P_0(II)$

Wet previous days $\quad P_0(III) = 0.43 \cdot P_0(II) \quad$ for P_0 (II)>35

$P_0(III) = 0.0072 \cdot P_0(II)^2 + 0.167 \cdot P_0(II) \quad$ for P_0 (II)<35

Where:

P_0 (II) $\quad P_0$ for Antecedent Moisture Condition II (Normal)

P_0 (I) $\quad P_0$ for Antecedent Moisture Condition I (Dry)

P_0 (III) $\quad P_0$ for Antecedent Moisture Condition III (Wet)

The hydrological soil group also plays an important role in the initial abstraction. In the SCS method, these properties are represented by a hydrological parameter: the minimum rate of infiltration obtained for a bare soil after prolonged wetting. The influence of both the soil's surface condition (infiltration rate) and its horizon (transmission rate) are thereby included. This parameter, which indicates a soil's runoff potential, is the qualitative basis of the classification of all soils into four groups. (Chow V. et al., 1994) The Hydrological Soil Groups, as defined by the SCS soil scientists, are:

Group A: Soils having high infiltration rates even when thoroughly wetted and a high rate of water transmission. Examples are deep, well to excessively drained sands or gravels.

Group B: Soils having moderate infiltration rates when thoroughly wetted and a moderate rate of water transmission. Examples are moderately deep to deep, moderately well to well drained soils with moderately fine to moderately coarse textures.

Group C: Soils having low infiltration rates when thoroughly wetted and a low rate of water transmission. Examples are soils with a layer that impedes the downward movement of water or soils of moderately fine to fine texture.

Group D: Soils having very low infiltration rates when thoroughly wetted and a very low rate of water transmission. Examples are clay soils with a high swelling potential, soils with a permanently high watertable, soils with a clay pan or clay layer at or near the surface, or shallow soils over nearly impervious material.

The following table provides the initial abstraction values for the four types of soil and corresponding to the landuse units defined in this thesis.

Land use	**Soil Type**			
	A	**B**	**C**	**D**
Urban areas	1	1	1	1
Constructed areas with vegetation between 50-75%	24	14	8	6
Natural Pastures	24	14	8	6
Short meadows	60	24	14	10
Areas with poor vegetation	24	14	8	6
Badlands and/or erosive areas	15	8	6	4
Poor Forest	40	17	8	5
River bed	5	5	5	5

The final value for the initial abstraction has to be determined according to the spatial distribution of each land use class.

Land-Soil Unit	**Area A_0 (km^2)**	**Ao/At**	**Initial Abstraction P_0(III)**	**Ponded P_0 P_0*Ao/At**
Areas with poor vegetation	37.33	0.59	6	3.6
River bed	1.11	0.02	2	0.0
Constructed areas with vegetation between 50-75%	2.05	0.03	6	0.2
Badlands and/or erosive areas	8.70	0.14	3	0.5
Natural Pastures	7.67	0.12	6	0.7
Poor Forest	0.25	0.00	7	0.0
Short meadows	1.40	0.02	10	0.2
Urban areas	4.30	0.07	0	0.0
Total Area	**At = 62.81**		**Σ P_0**	**5.3**

The next step to calculate de effective rainfall is to calculate the accumulated rainfall $\sum P$, if this value is lower than the initial abstraction then the effective rainfall is zero, otherwise the effective rainfall is calculated using Eq.1applied to the accumulated rainfall.

$$\sum P_n = \frac{(\sum P - P_0)^2}{\sum P + 4P_0}$$

The final step is to calculate the difference between each consecutive accumulated effective rainfall in order to get the distribution of the effective rainfall along the rainfall period. Next table shows the effective rainfall calculated for this thesis.

Hours	**P (mm)**	**ΣP (mm)**	**ΣPn (mm)**	**Pn**
1	0.0	0.00	0.00	**0.00**
2	6.0	6.00	0.04	**0.04**
3	0.0	6.00	0.04	**0.00**
4	0.0	6.00	0.04	**0.00**
5	0.0	6.00	0.04	**0.00**
6	2.1	8.10	0.34	**0.30**
7	0.1	8.20	0.36	**0.02**
8	0.2	8.40	0.41	**0.04**
9	0.0	8.40	0.41	**0.00**
10	0.0	8.40	0.41	**0.00**
11	1.5	9.90	0.80	**0.40**
12	0.2	10.10	0.86	**0.06**
13	0.2	10.30	0.93	**0.06**
14	0.1	10.40	0.96	**0.03**
15	0.3	10.70	1.06	**0.10**
16	0.2	10.90	1.13	**0.07**
17	0.1	11.00	1.16	**0.03**

APPENDIX 4 Potential regression

A potential equation has the following expression: $F_p = K \cdot t^{\alpha}$

Where K and α are the unknown parameters.

F_p is the accumulated infiltration (mm)

t is time (min)

For the problem under analysis, the linear regression can be made applying logarithms to both sides of the equation

$$\log F_p = \log K + \alpha \log t$$

The objective is to find the values for K and α. In order to obtain these values the following expressions are used.

$$\sum \log F_p = N \log K + \alpha \sum \log t$$

$$\sum (\log F_p \log t) = \log K \sum \log t + \alpha \sum \log t^2$$

$\Sigma \log F_p$ = Sum of the infiltration rate logarithm

N = Number of records

Log K = logarithm of coefficient K

α = slope of the curve

Σlog t = Sum of the accumulated time logarithm

Σ (log fp * log t) = Sum of the product between the infiltration rate logarithm and the accumulated time logarithm

$\Sigma \log t^2$ = Sum of the logarithm of the square accumulated time

These two equations correspond to a linear equation system with two unknown parameters. Isolating Log K from both of them

$$\log K = \frac{\sum \log F_p - \alpha \sum \log t}{N} \quad \text{and} \quad \log K = \frac{\sum \log F_p \sum \log t - \alpha \sum \log t^2}{\sum \log t}$$

From these two equations

$$\alpha = \frac{N \sum \log F_p \log t - \sum \log t \cdot \sum \log F_p}{N \sum \log t^2 - (\sum \log t)^2}$$

$$\log K = \frac{N \sum \log t_2 \sum \log F_p - \sum \log t \cdot \sum \log t \log F_p}{N \sum \log t^2 - (\sum \log t)^2}$$